Development of a novel active targeting system for siRNA delivery to liver sinusoidal endothelial cell in vivo

(肝臓類洞内皮細胞へのsiRNA送達を目的とした革新的な能動的標的化システムの構築)

A Dissertation
Submitted To

The Graduate School of Life Science
Hokkaido University
In Partial Fulfillment of the Requirements
For The Degree of
Doctor of Philosophy

Laboratory of Innovative Nanomedicine
Department of Biomedical and Pharmaceutical Science
Graduate School of Life Science
Hokkaido University
Hokkaido, Sapporo, Japan

Afsana Akhter
September 2013

Development of a novel active targeting system for siRNA delivery to liver sinusoidal endothelial cell in vivo

A Dissertation
Submitted by

Afsana Akhter

In partial fulfillment of the requirements for the Degree of
Doctor of Philosophy in
Pharmaceutical Sciences

(Faculty of Pharmaceutical Sciences)
Hokkaido University
Hokkaido, Sapporo, Japan
2013

Supervisor
Prof. Dr. Hideyoshi Harashima

Review Committee
Prof. Dr. Mitsuru Sugawara
Associate Prof. Dr. Yoh Takekuma
Associate Prof. Dr. Hidetaka Akita

Dedication

To my beloved Parents

Acknowledgements

First I would like to express my deepest thanks to my supervisor Prof. Hideyoshi Harashima for accepting me as a graduate student in his laboratory. I am also indebted to him for providing me the opportunity to complete my PhD thesis. He has been so supportive since the days I began working. Ever since, his patience, motivation, enthusiasm, and immense knowledge always inspired me to continue my study. He has been actively interested in my work and has always been available to advise me. Thanks to him for giving me the opportunity to conduct my research career in the field of Nanotechnology. His guidance will be the key to take the challenges as well as to build up my future career.

This work would not have been possible without the encouragement and guidance of Dr. Yasuhiro Hayashi, former member of this lab. Words are too short to represent his countless efforts to teach me the basic things that I required for my research, generate new ideas and to get good results. Lot more thanks to him for intellectual brilliance and encouragement. Since the first day of our introduction, to all the way towards my research, he provided me the support I needed at every step. It is his careful supervision that brought me wherever I stand today in my research career. Thank you for your kind assistance and insight on completing this paper.

I also want to express my deep gratitude to Dr. Yu Sakurai for his continuous suggestion not only in writing this thesis paper but also in experimental works. I am also expressing my appreciation to Dr. Hidetaka Akita, Dr. Kazuaki Kajimoto, Dr. Yuma Yamada, Dr. Hiroto Hatakeyama, Dr. Mamoru Hyodo, Dr. Takashi Nakamura, for their advice during my study.

I am grateful to Dr. Kyoko Hida and Dr. Noritaka Ohga, Division of Vascular Biology, Graduate School of Dental Medicine, Hokkaido University for their kind assistance; especially for the liver endothelial cells that I used in my research.

My sincere thanks also go to the members of my doctoral committee for their input, valuable discussions and suggestions. I am expressing my gratitude to Prof. Mitsuru Sugawara, Laboratory of Pharmacokinetics, Hokkaido University, who was the

Chairman in my doctoral thesis presentation. I am also thankful to the reviewers of my thesis paper for their kind observations and expert opinions.

I want to thank present and past members of the lab: Chisato Nagai, Jun Yamauchi, Mina Tamaru, Naoyuki Toriyabe, Yuki Noguchi, Erina Suemitsu for giving me the introductory lessons about the lab and for sharing their knowledge.

I am also expressing my gratefulness to the Staff of Faculty of Pharmaceutical Sciences, Hokkaido University for their response to me; whenever I go to them they always welcome and support me. Very special thanks to Eiko Abe who made all the administrative issues easier for my stay in Japan.

My deepest gratitude goes to my family for their continuous love and support throughout my life; this thesis is simply impossible without them. I am indebted to my father, Muhammad Nasir and mother, Raihana Begum; for the love and support they have provided throughout my entire life. They have never complained in spite of all the hardships in their life. I am ever grateful to their unselfish blessings and supports. I also want to thank my brother Rakibul Hasan and my in-law parents for their faith and mental supports.

Finally, and most importantly, I would like to thank my husband Dr. Golam Kibria for his untiring support, encouragement, patience and love, which strengthen me to go ahead to my future dream. I am expressing my deepest love and affection to my son Tajwar Morshed (Ayaan), whose presence in my life strengthened me to take every challenges of life . This work would not come true without their sacrifices.

Above all I want to give thanks the omnipresent Allah, for answering my prayers for giving me the strength to finish this thesis work in time.

TABLE OF CONTENTS

Page

Page

Formulation of new peptide-conjugated MEND and delivering siRNA to LSEC

. Aim of the study

Liver sinusoidal endothelial cell (LSEC) has become an interest of study for some recent years as it plays some important role in both physiological and pathophysiological condition. On the basis of this consideration the main aim of this study was to develop a peptide modified MEND that can be extended for systemic in vivo application for intracellular delivery of small-interfering RNA (siRNA) to LSEC. The different specific steps on the way to achieve this aim are the following:

- To design an LSEC targeting peptide ligand to develop an LSEC targeting nanocarrier

- To design a liposomal carrier modified with the designed ligand and to check the target efficiency of the developed carrier

- To develop a successful MEND modified with the specific ligand for siRNA delivery to LSEC

- To check the specificity of the developed MEND to deliver an endothelial cell specific gene suppressing siRNA to LSEC

- To optimize the MEND for in vivo application through modification of the functional device attached on the MEND surface and to study the mechanism of the endosomal escape of the developed MEND into LSEC

- Finally to check the safety profile data of the developed nanocarrier for in vivo siRNA delivery

1

General Introduction

1.1. Liver

The liver is considered as the most important organ present in animal body. It has numerous metabolic functions, such as, metabolism of carbohydrates, proteins and fats. It also works as a storage site of Vitamins and Iron [1]. Besides metabolism liver also plays important role in the defense mechanism of human body by detoxification of bloods by removing toxic elements, drugs, hormones and other substances [1]. Diffense mechanism in liver is usually carried out by sinusoidal endothelial cell. Liver Sinusoidal

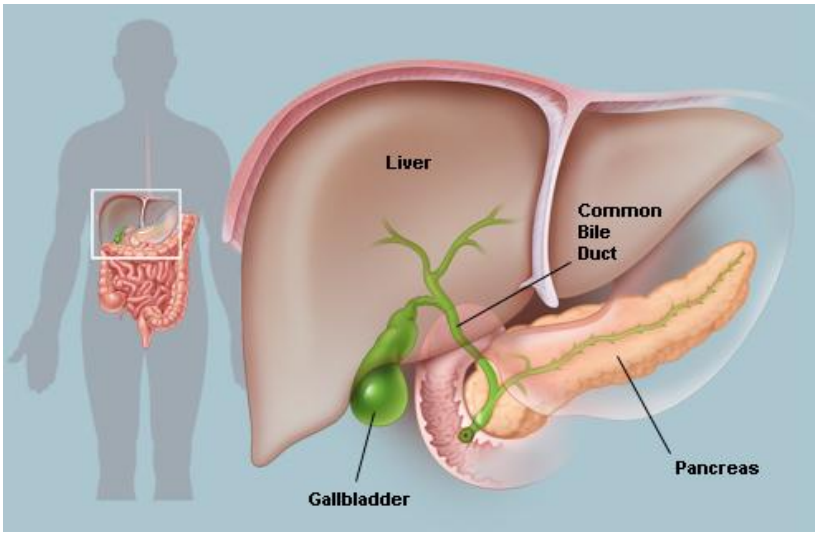

Figure 1.1: Liver-An important power and sewage treatment plant of animal body (Ref: Encyclopedia of Britanica)

endothelial cells (LSECs) can take up an array of different substances by receptor mediated endocytosis. This feature of LSEC reflects their important role as a scavenger system that clears the blood from many different macromolecular waste products [2]. As a part of innate immunity system under normal conditions LSECs employ only receptor-mediated endocytosis to eliminate soluble or colloidal substances [3]. In

diseased condition this endothelial cells also plays important role in inflammatory condition by transmigration of inflammatory cells to non parenchymal cells [4]. Endothelial cells can also act as second line defense in the liver to remove foreign materials from the blood when Kupffer cells phagocytic function is totally disturbed [2]. On the basis of studies on the role of LSEC in the diffense mechanism of liver in diseases stage, in this study an attempt was made to develop a drug carrier targeting LSEC to deliver a drug exploiting the high endocytic capacity of LSEC.

1.2. Structure of liver

Human liver is primarily consists of two lobes and many lobules. The lobules consist of parenchymal cells, blood sinusoids and bile ducts. Liver sinusoid harbors 4 different cells [5]:

- Endothelial cells
- Kupffer cells
- Stellate cell

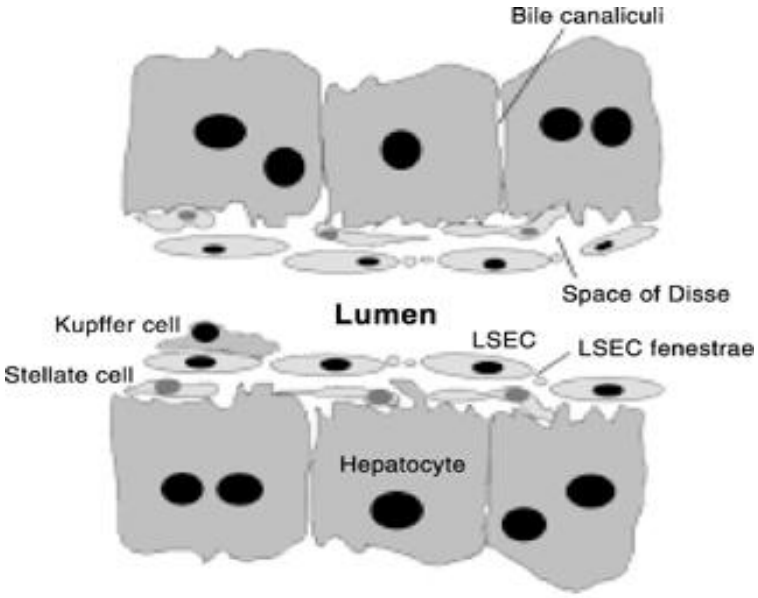

- Natural killer cell (Pit cell)

Figure 1.2: Schematic structure of the liver sinusoidal endothelium [5]

Some special features of liver sinusoids are given below [5]:

- Liver sinusoids are lined by liver sinusoidal endothelial cells (LSEC)
- LSECs are fenestrated and the fenestrae are lacking of diphrahm
- LSEC separate the sinusoid lumen from hepatocytes
- Kupffer cells patrol the sinusoids and bind to LSEC and occasionally hepatocytes through the gaps of two adjacent LSEC
- Stellate cells are located in the space of Disse.

1.3. Different types of cells in liver and their function

As we described in *section 1.2* there are different types of cells present in liver. Each cell type has their unique features and function.

Hepatocytes

Eighty percent liver cells are parenchymal cells which are also known as hepatocytes. Hepatocytes participate in the metabolism of proteins, glycides, lipids, metals and vitamins. They also participate in the processes of excretion, detoxification and storage of energy. These cells also excrete various mediators acting in paracrine interactions, which may affect functions and communication with distant non-parenchymal cells.

Sinusoidal Endothelial cells

Endothelial cells are the major non-parenchymal cells and they mediate communication between hepatocytes and inner space of sinusoids, as well as prevent pathogen infiltration into the liver parenchyma [6].

Kupffer cells

Kuppfer cells are liver macrophages. These cells are activated by gut-derived bacterial endotoxins, which are characterized by high phagocytic, endocytic and secretory activities [6].

Hepatic stellate cells (HSC)

HSC usually perform as a storage cell for vitamin A and lipid. Upon liver damage, these

cells participate in initiation and progression of liver fibrosis and thus may contribute to the development of liver cancer [6].

Pit cells

Pit cells have characteristic features of natural killer cells (NK) and they exert their cytotoxic activity against tumor cells [6].

Besides these functions the cells within sinusoids also contribute in the exchange of metabolites between plasma and hepatocytes, degradation of toxic particles, such as microbial agents or cellular debris. They took part in blood flow regulation.

1.4. Biological features of liver sinusoidal endothelial cell (LSEC)

LSECs develop the wall of the liver sinusoids that carry blood throughout the liver. They separate the hepatocytes from the blood flowing through the sinusoids and play an important role in hepatic microcirculation. LSECs form a continuous, but fenestrated lining of the hepatic sinusoids [7]. Figure 3 shows rat liver endothelial lining as seen by scanning electron microscopy. The fenestrae are grouped in sieve plates. Fenestrae have an average diameter of about 150 nm to 175 nm. Fenestrae filter fluids, solutes and particles that are exchanged between the sinusoidal lumen and the space of Disse. Particles smaller than the size of fenestrae reaches to parenchymal cells and the larger ones remain in the space of Disse.

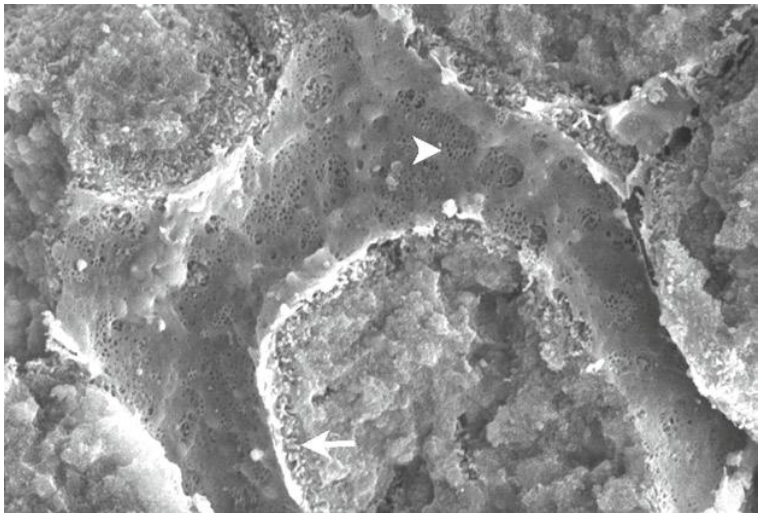

Figure 1.3: Scanning electron microscopy picture of hepatic sinusoid. Arrow head indicates a sieve plate in the LSEC. Arrow indicates hepatocyte villi in the space of Disse.

1.5. General functions of LSEC

LSECs have a number of important functions. The major functions have been summarized below [9, 10]:

(1) LSECs act as a porous barrier which facilitates oxygenation of hepatocytes and enhances hepatocyte exposure to macromolecules in the portal circulation
(2) They mediate communication between hepatocytes and inner space of sinusoids
(3) LSEC also can act as scavengers, eliminating soluble waste macromolecules from portal venous blood
(4) They also acts as gatekeeper against hepatic stellate cell (HSC) activation

1.6. Phenotype of LSECs;

Although there are a number of surface markers present on LSEC (Table 1), only a few of them are specific for LSEC within the liver [11-15].

Table 1.1: Selected markers present on LSEC

Markers	**Functions**
CD31	Functions in cell adhesion and signalling
Von Willebrand Factor (vWF)	A multimeric glycoprotein that binds and stabilises the coagulation factor FVIII as well as supports the adhesion of platelets to subendothelial structures during vascular damage.
E-Selectin	Adhesion molecules that supports leukocyte binding. Expression of E-selectin is restricted to vascular endothelial cells in the normal liver.
Ulex lectin	Used as a histological marker for endothelial cells
Pal-E Antigen	The antigen recognised by the Pal-E antibody is a widely used marker of vascular endothelial cells
Vascular Endothelial-Cadherin (VE-Cadherin)	Adhesion molecules that demonstrate cation- dependent homophilic and heterophilic binding.
CD105/endoglin	CD105 (endoglin) is a hypoxia-inducible protein that is widely expressed on endothelial cells and is upregulatedduring angiogenesis.
Stabilin -2 (also known as hyaluronan receptor)	Main scavenger receptor on LSEC, thought within the liver to be unique for LSEC
Integrin α1ß1	Preferentially binds with collagen IV
Integrin α5ß1	Binds with fibronectin
Some other markers reported on LSEC are LYVE-1 (another scavenger receptor,expressed only on liver cells), ICAM-2, CD46, CD80, CD-86, LRP-1 etc.	

1.7. Morphology of LSEC

1.7.1 Fenestration

Liver sinusoids can be regarded as unique capillaries in the body because of the presence of pores. These pores are termed as fenestrae. The first description and electron microscopic observation of LSEC fenestrae was given by Wisse in 1970 [7]. In general, endothelial fenestrae size ranges from 150–175 nm in diameter and they occupy 6-8% of the endothelial surface. Fenestrae filter fluids, solutes and particles. They exchange particles between the sinusoidal lumen and the space of Disse. Fenestra allows exchange of particles which are smaller than the size of fenestral diameter. [16.]

1.7. 2. Contraction and dilatation mechanism of fenestrae

In 1986 it was first assumed that a calcium-calmodulin-actomyosin system around fenestrae is playing the major role in the regulation of the size of the fenestrae [17, 18]. Addition of a calcium ionophore to LSEC induced fenestral contraction [19]. This contraction could be suppressed by extracellular calcium or by pretreatment of LSEC with a calmodulin antagonist, demonstrating the messenger function of calcium ions and the role of the intracellular Ca2+-receptor calmodulin in the fenestrae diameter regulation. In addition, it was also demonstrated that serotonin induces contraction of fenestrae with phosphorylation of myosin light chain kinase [20]. All these findings are suggesting the role of calcium- calmodulin-actomyosin complex in the regulation of fenestral diameter (Fig. 4) [21]. Serotonin induced fenestral contraction is associated with an increment of intracellular calcium, using a serotonin-sensitive cation channel with permeability to calcium [22].

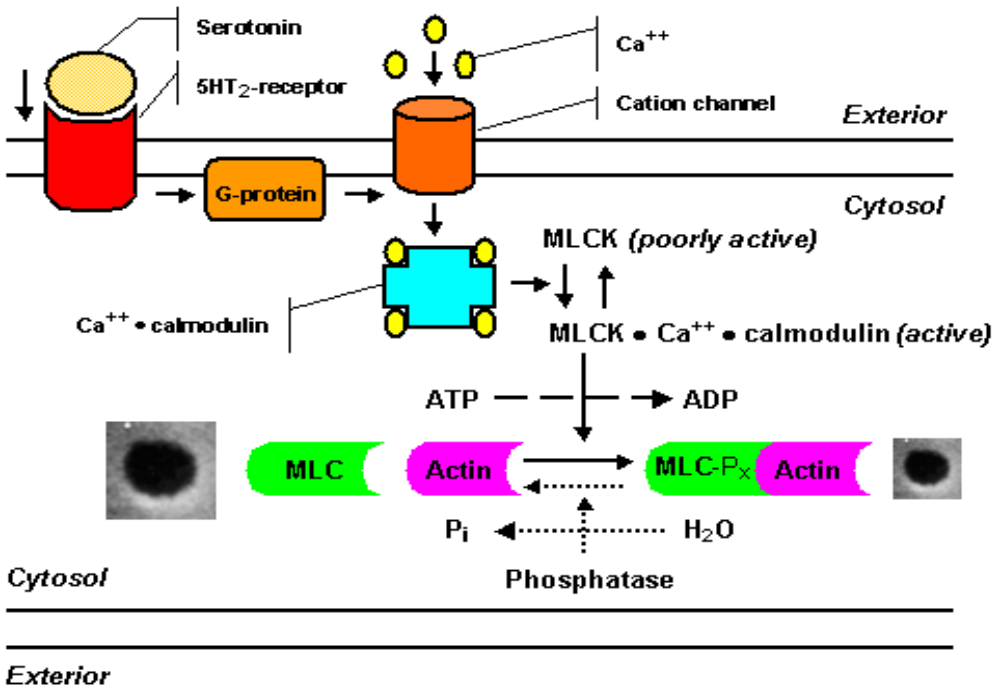

Figure 1.4: Scheme of the serotonin signal pathway showing the steps in fenestral contraction and relaxation [21].

1.8. Liver Diseases and LSEC

Liver diseases which are related with LSEC injury are as follows [7]:

Table 1.2: Diseases related with LSEC dysfunctions

Hepatitis
Fibrosis
Cirrhosis
Alcoholic liver disease
Sinusoidal obstruction syndrome
Radiation-induced liver disease
Ischemia–reperfusion injury
Heterogeneous liver perfusion
Peliosis hepatitis

1.8.1. Hepatitis

Liver is the main target organ of many infectious diseases, especially infections caused by hepatitis viruses. It was reported that in animal hepatitis B virus (HBV) models, the virus was taken up by liver sinusoidal endothelial cells, rather than hepatocytes [23]. It is recently demonstrated that T_{LSEC} inhibited the proliferation of native CD4+ T cells in vitro although being $CD25^{low}$ and lacking expression of forkhead box protein (FoxP)3 which ultimately suppresses autoimmune hepatitis [24]. In vitro co-culture of LSEC and hepatocytes reduced the permissivity of hepatocytes to support hepatitis C virus (HCV) replication [25]. Importantly, recombinant VEGF did not show any affect on HCV replication in hepatocyte monocultures, which suggests that that VEGF stimulates endothelial cells to modulate expression of molecules that regulate hepatocyte permissivity to HCV infection [25]. All these data indicates that LSECs plays important role not only in the uptake of virus causing hepatitis but also in the progression of diseases.

1.8.2. Cirrhosis and Fibrosis

Cirrhosis is described as a diffuse process characterized by fibrosis and abnormal nodules in liver [26]. Hepatic fibrosis develops in most chronic liver diseases as a precursor of cirrhosis. Alcohol and some other chemical toxins exposure cause fibrosis and cirrhosis [16]. Although there are many causes and morphologies of hepatic cirrhosis, all forms of cirrhosis are characterized by a defenestrated sinusoidal endothelium and the presence of a subendothelial basement membrane [16, 27]. In cirrhotic livers defenestratration causes impaired exchange of different particles between sinusoidal blood and hepatocytes [28,29]. Further involvement of LSEC has been described in chapter-2.

1.8.3. Sinusoidal Obstruction Syndrome (SOS)

A sinusoidal obstruction disease occurs due to the damage of liver sinusoidal endothelial cells. The damage usually occurs due to exposure to pyrollizidine alkaloids or drugs like actinomycin D, azathioprine, busulfan etc. [9]. The possible mechanism for occurring SOS is given below [9].

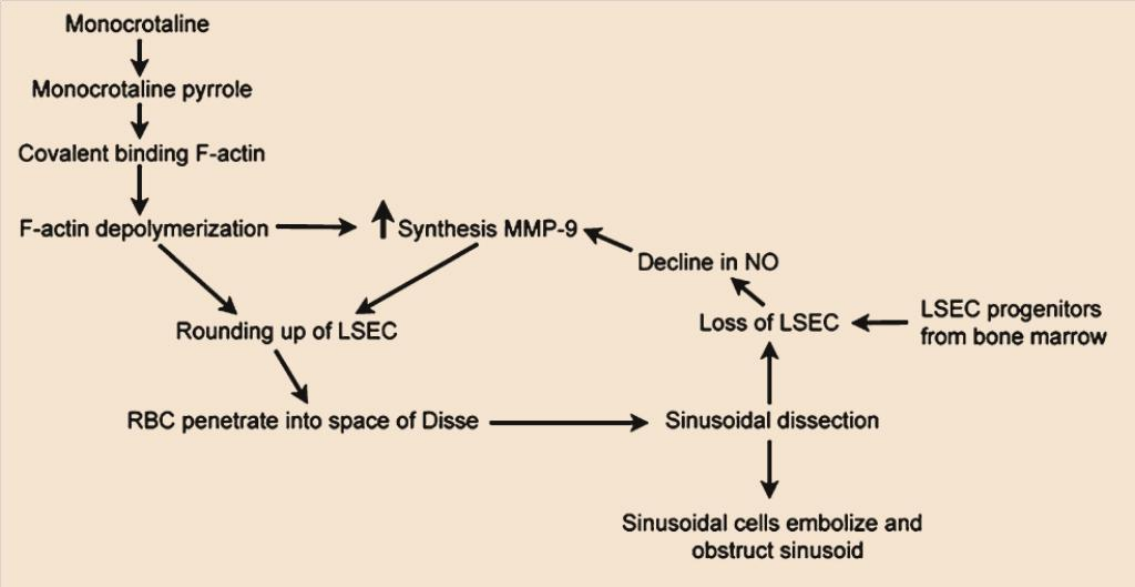

Figure 1.5: Possible mechanism of SOS and involvement of LSEC. Here, MMP-9: matrix metalloproteinase-9 and NO: nitric oxide

1.8.4. Radiation-Induced Liver Disease (RILD)

RILD occurs in patients who undergo irradiation for primary or metastatic cancer in the liver. RILD develops due to endothelial damage in liver sinusoid [9]. Histological features of RILD are sinusoidal hemorrhage and congestion, fibrotic veno-occlusive lesions of the central vein sometimes accompanied with the portal veins, and centrilobular atrophy [9].

1.8.5. Alcoholic Liver diseases (ALD)

Alcoholic liver disease (ALD) encompasses a spectrum of injury, ranging from simple steatosis to cirrhosis. As compared to non-alcoholics a significant decrease in the number of porosity in liver sinusoid is observed in patients suffering from alcoholic liver diseases [30]. Chronic Alcohol abuse induces a decrease in the number of fenestrae in rats resulting in decreased porosity in liver sinusoids [31]. Probably hyper lipoproteinemia causes simultaneous decrease in the porosity of the liver sieve [32]. These data proves involvement of LSEC in Alcoholic liver diseases.

1.9. Pathophysiology of liver diseases

As described in the section 1 the main function of the liver is metabolism as well as playing important role in the defense mechanism. It protects our body by taking up various toxic drugs, microorganisms and other toxins from microcirculation. As a clearance organ, liver is always at the risk of exposure to toxic substances which may lead to liver injury. Both parenchymal and nonparenchymal cells of livers takes part in defense mechanism. Among the nonparenchymal cells Kupffer cells, sinusoidal endothelial cells, and natural killer (NK) cells takes major part in defense functions of liver.

1.9.1. Inflammation and other liver injury

In the early stage of any liver diseases it may become inflamed. Inflammation shows that body is trying to fight against any infection or injury. Even the word 'hepatitis' means 'inflammation of liver'. In acute hepatitis inflammation is usually caused by different types of noxae. But if the inflammation continues over time, it can start to cause permanent damage of liver. Hepatic fibrosis is the common endpoint of chronic liver inflammation. It is considered as an irreversible process. When liver is exposed to any infectious microbe or toxic products then first it tries to eliminate that harmful products, but when it fails to do so then inflammation and fibrosis occurs [33].

Acute hepatitis caused due to viral infection is usually followed by complete recovery [33]. But chronic infection of liver due to hepatitis B and C leads to inflammation followed by death of hepatocytes and fibrosis. Incase of chronic hepatitis C infection up to 20% of patients will develop long-term sequelae, such as cirrhosis and hepatocellular carcinoma, over a period of 20 years [34]. The severe pathological consequences of persistent hepatitis B infections (HBV) may lead to development of chronic hepatic insufficiency, cirrhosis, and hepatocellular carcinoma (HCC) [35]. Injury from HBV is due to immune-mediated damage to infected hepatocytes [36].

In alcoholic hepatitis, sinusoidal fibrosis leads to rapid development of cirrhosis, with the liver extensively subdivided by sub lobular fibrous septa developed in the midst of extensive inflammation and hepatocellular destruction [37]. After development of

cirrhosis continuous destruction of the parenchyma may produce a densely fibrotic organ with little remaining parenchyma. Hepatic inflammation may also mediate fibrogenesis in patients with liver steatosis [34].

1.9.2. Chemokines and cytokines

Cytokines (Greek cyto-, cell; and -kinos, movement) are small signaling molecules used for cell signaling. There are different types of cytokines which can be classified as proteins, peptides or glycoproteins. Actually all cell types produces cytokines but specially endothelial, epithelial cells and resident macrophages are the major types of cells that secretes cytokines.

Chemokines (Greek -kinos, movement) are a family of small cytokines or signaling proteins that are secreted by cells. Chemokines are a family of chemotactic cytokines that play important roles in inflammatory responses. They are classified into four main subfamilies: CXC, CC, CX3C and XC. All these proteins exert their biological effects by interacting with transmembranal G protein-linked receptors. These receptors are also called as chemokine receptor. Chemokines are expressed on the surface of the target cells.

CXC chemokines are a group of molecules that have pro-inflammatory property and are produced by many cell types, including hepatocytes [38]. Members of this family include platelet factor 4 (PF-4), growth-related oncogene alpha, beta, and gamma, epithelial neutrophil activating protein (ENA-78), interleukin-8 (IL-8), granulocyte chemotactic protein-2, connective tissue-activating protein-III, beta thromboglobulin, neutrophil activating protein-2, gamma interferon- inducible protein (IP-10), and monokine induced by gamma-interferon (MIG) [38]. It has been reported that when the defense mechanisms are not sufficient to withstand the damaging attacks cells start to synthesize chemokines-induced by gamma interferon (MIG) and gamma-interferon-inducible protein (IP-10) [38]. During inflammation cytokine-induced neutrophil chemoattractant (KC) and macrophage inflammatory proteins (MIPs) are also increased (figure-6) [39]. MIPs and KCs are considered to be responsible for attraction of inflammatory cells like granulocytes and mononuclear phagocytes and to

activation of resident macrophages.

Another group of chemokines named as CXCL9 is differentially expressed in fibrosis-susceptible and fibrosis-resistant mice and this CXCL9 has antifibrotic effect [39]. This data set the stage for further evaluation of other chemokine system as a potential antifibrotic target. A list of chemical mediators during inflammation has been given below [33]:

Table 1.3: List of chemical mediators secreted by different types of liver cell

Liver cells	Mediators
Hepatocytes	IL-8, IP-10, MIG, MIP-1, MIP-2, MIP-3, KC
Sinusoidal endothelial cells	RANTES, MCP-1, IL-8, MIP-1α, MIP-1ß, MIG, ITAC
Kupffer cells	IL-1, IL-6, IL-10, IL-18, TNF-α, TNF-ß, MIPs, IL-8, IP-109, KC/GRO, RANTES
Hepatic stellate cells	IL-8, RANTES, MCP-1

1.10. Role of different types of cells in liver inflammation

1.10.1. Role of hepatocytes

Hepatocytes make upto 70-80% of the cytoplasmic mass of the liver [33]. These cells are involved in synthesis and storage of protein, transformation of carbohydrates, synthesis of cholesterol, bile salts and phospholipids, and detoxification. Hepatocytes are organised into plates and separated from blood flow by a thin layer of sinusoidal endothelial cell [41]. Induction of inflammation both in vitro and in vivo causes chemokine production by hepatocytes [42]. Several cytokines and growth factors have been shown to regulate chemokine gene expression in hepatocytes [42]. Such cytokines (interleukins-(IL)-1 and -6, tumor necrosis factor-alpha (TNF-alpha) and interferon-gamma) are released during the acute-phase reaction [43, 44]. Hepatocytes synthesize cytokines like interleukin (IL)-8 and respond to acute phase mediators like IL-6, with the synthesis of acute phase proteins like C-reactive protein (CRP) [42].

1.10.2. Role of Sinusoidal endothelial cells

Hepatits causes increased expression of the pro-inflammatory chemokines CXCL9 and CXCL10 by liver [45]. LSEC internalized basolateral CXCL9, CXCL10 and CXCL12 via clathrin-coated vesicles and thus increases transmigration of inflammatory cells to hepatocytes. Inhibition of endothelial chemokine transcytosis suppressed chemically induced hepatitis by preventing tissue immigration of T cells, particularly chemokine-responding CXCR3+CD4+ T cells [45]. Thus, chemokine presentation by LSEC during liver inflammation might be a promising therapeutic target in hepatitis.
Under normal conditions the hepatic sinusoidal endothelial cells express different types of chemokines like RANTES, IL-8, MCP-1 and MIP-1 [33]. These factors are involved in the routine leukocyte recirculation and immunological surveillance. During inflammation the chemokine expression profile of the normal hepatic endothelium changes. These changes are characterized by expression of high levels of MIP-1ß, IP-10, MIG and IFN-gamma-inducible T cell alpha chemoattractant (ITAC) [33]. LSECs also increases the production of cytochemokines due to excessive alcohol [46].

Liver inflammation also changes the expression profile of adhesion molecule expression by LSEC. In diseased human livers platelet endothelial cell adhesion molecule-1 (PECAM-1) was detectable along the sinusoids, within inflammatory infiltrates and within fibrotic area [47]. In diseased liver expression level of intracellular cell adhesion molecule-1 (ICAM-1) and vascular cell adhesion molecule-1 (VCAM-1) increases with the decrease in the expression level of PECAM-1 [47].

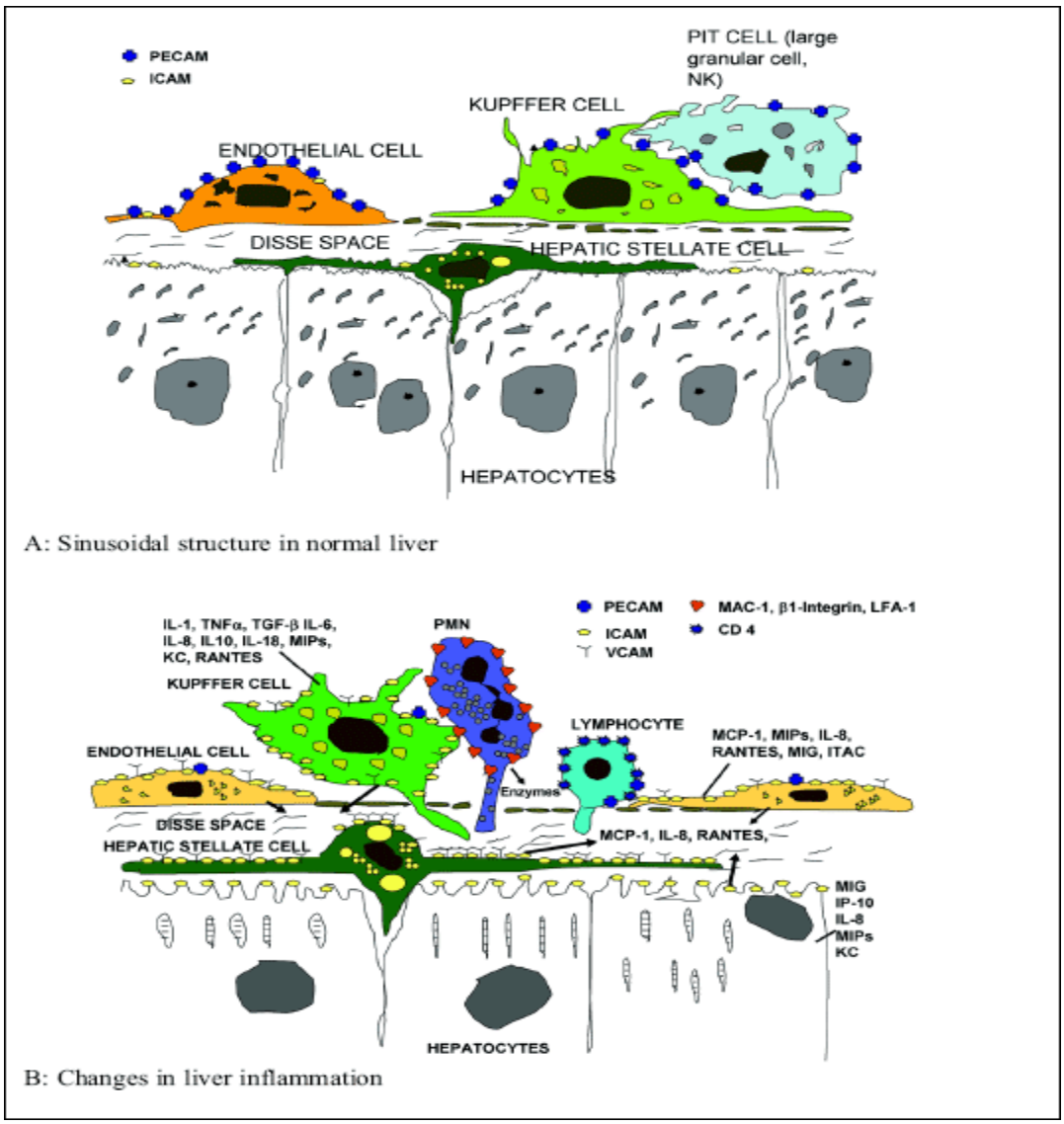

Figure 1.6. Schematic representation of sinusoidal structure in normal liver (A) and in liver inflammation (B). The model shows that hepatotoxins induces activation of pit cells and Kupffer cells which increases production of VCAM-1 and ICAM-1 in LSECs and down regulation of platelet endothelial cell adhesion molecule (PECAM-1). These molecules are responsible for the recruitment and sinusoidal transmigration of inflammatory cells toward their target, the hepatocyte [33].

1.10.3. Role of hepatic stellate cells

Hepatic stellate cells (HSC) are considered as the principal matrix-synthesizing cells of fibrotic liver. They might also play a role in liver inflammation. Growth factors, eg, transforming growth factor-alpha 1, causes the down-regulation ICAM-1 and VCAM-1 coding mRNAs and stimulated NCAM expression of HSC at inflammatory conditions whereas induction of ICAM-1 and V-CAM-1 specific transcription was increased several fold [48].

1.10.4. Role of Kupffer cells

Kupffer cells are considered as the specialized macrophages of the liver that form the major part of the reticuloendothelial system (RES). In liver injury and hepatocellular necrosis activated Kupffer cells acts as a major source of inflammatory mediators including cytokines, chemokines, nitric oxide, eicosanoids, lysosomal and proteolytic enzymes and demonstrate increased cytotoxicity and chemotaxis [49]

Increased circulating levels of pro-inflammatory cytokines like TNFα and IL-6, and chemokines like IL-8, MCP-1 and MIP-1α have been detected in patients with alcoholic liver disease, which could potentially be related to Kupffer cell activation [49].

Kupffer cell-derived TGF-ß1 has been suggested to drive hepatic stellate cell transformation and to induce production of collagen and proteoglycans by these cells [49]. TGF-ß1 is considered as the main cytokine that drives fibrosis in various animal models of hepatic damage [49]. TNF-α, IL-1 and MCP-1, that are produced by activated Kupffer cells, are also mitogenic and chemoattractant for HSC [49].

1.11. siRNA delivery to Liver

Small interfering RNA (siRNA) also called short interfering RNA, is a chemically synthesized double-stranded RNA molecules having 20-25 base pairs in length, which is generally delivered to the target cell by either viral or non-viral delivery systems. Principally, siRNA provides its function by RNA interference (RNAi) activity.

1.11.1. Advantages of siRNA delivery

In the field of gene therapy, siRNA delivery approach has a potential therapeutic application in the treatment of several pathophysiological conditions including cancer, liver diseases, infectious diseases etc. The notable advantage of siRNA delivery is that it can efficiently interact with the target gene and due to which the expression of the specific gene, responsible for the disease, is suppressed and finally can cure the disease.

1.11.2. Challenges in siRNA delivery

Despite of a promising therapeutic application, there are some major drawbacks in siRNA delivery. It is a big challenge to deliver siRNA to the target organ which is due to systemic instability as well as the anionic behavior of siRNA [50]. Due to the anionic nature, free siRNA faces difficulties to pass through the cell membrane to transport into the cell cytosol which limits the application of siRNA. To overcome such obstacles in siRNA delivery to the target sites, delivery systems including the use of viral vector, non-viral vector, lipid based nanoparticles etc. are used [50, 51]. Though viral vector was being used widely for the delivery of siRNA but it suffers from non-specificity or long time side-effects. For this reason non-viral siRNA delivery system was introduced to increase target specificity but their serious barrier is poor cellular uptake and lysosomal degradation [52, 53]. Though there are several reports of successful delivery of this type of non-viral carrier system but those systems failed to achieve acceptable safety profile and satisfactory tissue delivery in vivo [54].

1.11.3. Recent approaches in the delivery of siRNA to liver

Though researchers are trying numbers of approaches to deliver siRNA to liver cells for the down regulation of gene expression of disease related specific genes, only few of them showed therapeutic advantages. As non-viral approach without carrier, to deliver siRNA to liver is limited to hydrodynamic siRNA delivery. By this approach a large volume of siRNA solution is injected via high pressure. Hepatocytes are the target of this method. There have been several reports of siRNA delivery to liver by using hydrodynamic tail vein (HTV) injection method. For example by reducing some apoptopic gene expression the incidence of fulminant hepatitis was reduced by usinf this method [55, 56].

To increase the target specificity carrier modified non-viral system such as liposomes is now the extensively studied approach to deliver siRNA to liver. Liposomes have been used for the delivery of nucleic acids for over 25 years since first demonstration of their ability to transport the preproinsulin gene to the liver [57]. Cationic liposomes replaced the use of neutral liposomes as it was difficult to incorporate anionic siRNA into neutral liposome [58].

siRNA complexed with cationic lipoplexes also successfully delivers siRNA to liver. DOTAP/ cholesterol liposomes complexed with HBV siRNA successfully reduced viral protein expression of hepatitis B [59]. As an advancement of such type of method some researchers modified the cationic lipoplexes with a ligand which increased the specificity of the carrier to their target site. Lactosylated DOTAP-siRNA lipoplexes is an example of such delivery which showed mark reduction of hepatitis C expression in the liver [60].

Another extensively studied form of liposomes for siRNA delivery in *in vivo* is the stable nucleic acid lipid particle (SNALP). These nanoparticles can encapsulate and deliver siRNA to the liver with very high efficiency. The first successful delivery of siRNA to liver by this carrier was the silencing of hepatitis B virus (HBV) RNA [61].

As mentioned in previous section that lysosomal degradation is one of the main barrier for achieving successful result of siRNA delivery, researchers were finding ways to minimize the barrier. A programmed packaging concept, in which various types of devices may be incorporated into nanoparticles to control their behaviour, was evolved to break this barrier [62, 63]. MEND, a multifunctional envelope-type nano device, was proposed based on this concept to delivery siRNA or plasmid DNA. Liposomes modified with highly cationic cell penetrating peptide (CPP) for example octaarginine (R8) can be internalized into cells via macropinocytosis which is less susceptible to lysosomal degradation and leads to high gene expression in vitro [64]. Researchers took the advantages of this approach and achieved successful gene delivery to liver by R8-GALA-MEND [65].

1.11.4. Liver sinusoidal endothelial cell targeted siRNA delivery

LSECs have high endocytic capacity and they gave unique feature of fenestration. They play important role in inducing inflammation during diseased state by releasing chemokines or cytokines and also by changing the secreting profile of cell adhesion molecule. The above characteristics of LSECs are making them a good target for gene delivery. A few approches was made for gene delivery to LSEC in vivo.

Though there is no successful *in vivo* report of siRNA delivery to LSEC, some carrier mediated non-viral approach was successful to deliver plasmid DNA or oligonucleotide (ODN) to LSEC. LSECs possess unique receptors that recognize and internalize hyaluronic acid (HA). This HA modified targeted poly-L-lysine grafted-HA/DNA complex was delivered to LSEC via receptor mediated endocytosis which successfully delivered gene inside the cell [66].

More studies are needed to develop LSEC targeted non-viral delivery system and check their feasibility for gene delivery.

2

Development of LSEC selective ligand modified liposomes

2.1. Introduction

Two major types of cells populate the liver, namely, parenchymal and non-parenchymal cells. Approximately 80% of the liver volume is occupied by parenchymal cells commonly referred to as hepatocytes [33]. Sinusoidal endothelial cells, Kupffer cells and hepatic stellate cells are examples of non-parenchymal cells. Different types of liver diseases are associated with different types of liver cells. For example viral hepatitis and alcoholic hepatitis are associated with hepatocytes. LSEC dysfunction is associated with a variety of liver diseases, including fibrosis, cirrhosis, and portal hypertension [67]. Defenestration of LSECs causes hyperlipidemia, because it becomes difficult for lipoproteins to reach hepatocytes [68]. Kupffer cells are associated with the progression of non-alcoholic steatosis and fibrosis. It has also been reported that hepatocellular stress caused by various diseases causes the release of different types of cytokines and chemokines by different types of cells (Discussed in chapter 1) which ultimately cause the transmigration of inflammatory cells towards their target, hepatocytes [33]. Therefore, a selective drug delivery system would be an ideal approach for achieving a subsequent efficient therapy for different types of liver diseases.

A group of certain basic proteins or peptides have the ability to inhibit the binding of low density lipoprotein (LDL) to its receptor protein [69]. This inhibition is caused by polycations interacting with the receptor. LDLs are associated with a negatively charged LDL receptor even though the net charge of this lipoprotein is also negative. This suggests that the net charge of the LDL is governed by the positive charge of the ApoB sequence. Two basic regions of similar size in ApoB-100 segments, namely 3147 through 3157 and 3359 through 3367 are part of the LDL receptor binding domain. This

ApoB heterodimer binds to the LDL receptor and also binds with Glycoseaminoglycans (GAGs) with an affinity similar to that between LDL and GAGs [70]. The ApoB-100 segment RLTRKRGLK (3359-3367) is a mediator of the association between LDL and arterial chondroitin sulfate-rich proteoglycan (CSPG) [71]. It has recently been reported that LSEC express low density lipoprotein receptor protein-1 (LRP-1) which is a member of the LDL receptor gene family [72, 73]. Another study has shown that LDL is taken up by both parenchymal and non-parenchymal cells [74].

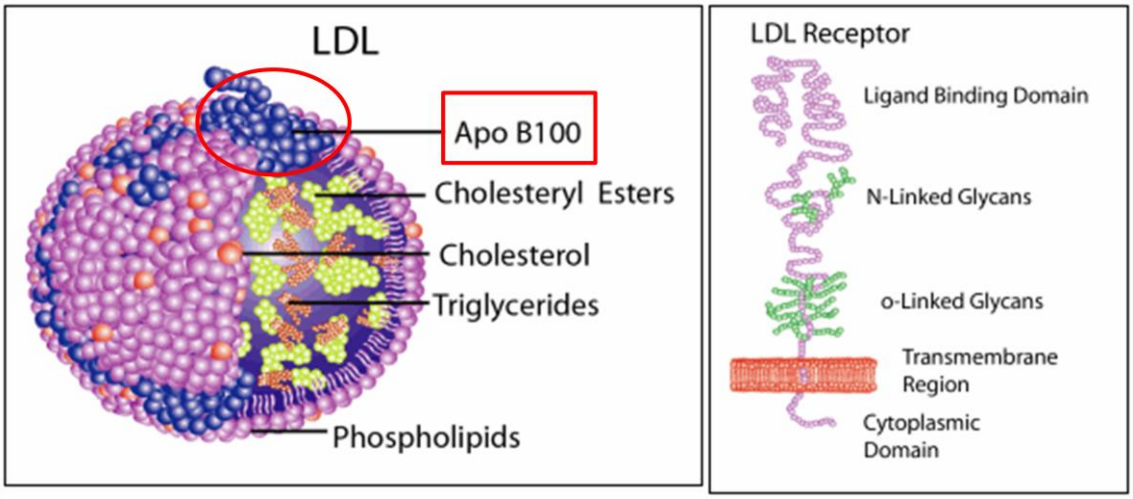

Figure 2.1: ApoB -100 in LDL molecule and LDL receptor

Liposomes are suitable nano-carriers that have the capacity to deliver drug particles to various target cells in vitro or diseased tissues in vivo [75, 76]. Based on these considerations, we selected the ApoB segment RLTRKRGLK (3359-3367) abbreviated here as RLTR for use as a novel ligand in designing a selective targeting system for hepatocytes. Surprisingly, however, this carrier system was accumulated through the blood vessels in the liver. In order to examine the targeting ability of this RLTR modified liposome, our effort was focused on two parameters, one being the cationic nature of this peptide and second the essential peptide sequence.

2.2. Materials and methods

2.2.1. Materials

Cholesterol (Chol), 1,2-dioleoyl-sn-glycero-3-phosphoethanolamine (DOPE), diethanolamine chloride (DC-6-14), Egg phosphatidylcholine (EPC), N-(lissamine rhodamine B sulfonyl)-1,2-dioleoyl-sn-glycero-3-phosphoethanolamine (rhodamine-DOPE), 1,2-distearoyl-*sn* -glycero-3-phosphoethanolamine-N-[methoxy (polyethyleneglycol)-2000] (PEG_{2000}-DSPE) were purchased from Avanti Polar Lipids (Alabaster, AL, USA). N-[(3-maleimide-1-oxopropyl) aminopropyl polyethyleneglycol-carbamyl] distearoylphosphatidyl-ethanolamine (maleimide-PEG-DSPE) was purchased from Nippon Oil and Fat Co. (Tokyo, Japan). ^{3}H-Cholesteryl hexadecyl ether (CHE) were purchased from New England Nuclear (USA). RLTRKRGLKGGC (RLTR in brief) and KLGRKRTLRGGC (KLGR in brief) peptides were purchased from Kurabo Industries, Osaka, Japan. Endothelial Cell Basal Medium (EBM-2) and other related growth factors were purchased from Lonza (Walkersville, MD, USA). Dulbecco's fetal bovine serum (FBS) was obtained from Hyclone Laboratories (Logan, UT, USA). All other chemicals used in this study were of analytical grade.

2.2.2. Animals

4-5 week old male ICR mice were purchased from Japan SLC (Shizuoka, Japan). The experimental protocols were reviewed and approved by the Hokkaido University Animal Care Committee in accordance with the guidelines for care and use of Laboratory animals. Animals were used without fasting in all experiments.

2.2.3. Conjugation of the RLTR peptide to PEG_{2000}-DSPE

Conjugation was achieved by incubating a 1.2:1 molar ratio of RLTRKRGLKGGC peptide and maleimide-PEG-DSPE in deionized water at room temperature for 24 hrs. The conjugation of RLTR with PEG was confirmed by matrix assisted laser desorption/ionization-time of flight (MALDI-TOF) MS (Bruker Daltonics, Germany) using acetonitrile: water=7:3 with 0.1 % of trifluoroacetate as the matrix solution, supplied with a 10 mg/ml solution of dihydroxybenzoic acid.

2.2.4. Preparation of liposomes

Liposomes (LPs) composed of EPC/Chol (molar ratio: 7/3) prepared by the lipid hydration method was used as control liposomes. Cationic LPs was prepared using DC6-14, DOPE, and Cholesterol at a molar ratio of 4:3:3 [77]. RLTR peptide modified PEG-LPs (RLTR-PEG-LPs) were prepared by adding the required amount of RLTR-PEG to the lipid solution. 1 mol% Rhodamine-DOPE was incorporated, to serve as a label for the lipid component. A lipid film was formed by evaporation of the solvents (chloroform and ethanol) from a lipid solution in a glass tube. HEPES buffer (10 mM, pH 7.4) was added and the solution was incubated for 10 min to hydrate the lipid film. The glass tube was then sonicated for approximately 30 sec in a bath-type sonicator (AU-25C, Aiwa, Tokyo, Japan). The mean size and zeta potential of the prepared LPs were determined using a Zetasizer Nano ZS ZEN3600 instrument (Malvern Instruments Ltd., Worchestershire, UK).

2.2.5. Isolation of Primary liver endothelial cells (LSECs)

LSECs were isolated as previously described [78, 79, 80]. Briefly, the liver of a female KSN mouse was excised. The excised tissue was minced and digested with collagenase II (Worthington, Freehold, NJ). Blood cells were removed by a single sucrose step-gradient centrifugation with Histopaque 1077 (Sigma-Aldrich), and the resulting cell suspension was filtered. Endothelial cells were isolated using MACS according to the manufacturer's instructions using a FITC-anti-CD31 antibody. CD31-positive cells were sorted and plated on 1.5% gelatin-coated culture plates and grown in EGM-2MV (Clonetics, Walkersville, MD) and 10% fetal bovine serum. After subculturing for 2 weeks, the isolated EC were purified by a second round of purification using FITC-BS1-B4 (Vector Laboratories, Burlingame, CA). All of the endothelial cells were split at a ratio of 1:3.

2.2.6. In vitro Cellular uptake study

For the cellular uptake study, 40,000 cells were seeded in a 24-well plate (Corning incorporated, Corning, NY, USA) (40,000 cells/well). After 24 hrs, the prepared rhodamine labeled PEG-LPs/ RLTR-PEG-LPs were added and incubated for an additional 3 hrs. After the incubation, the cells were washed with PBS (pH 7.4) and

then treated with Reporter Lysis Buffer (Promega Corp., Madison, WI, USA) followed by centrifugation at 12,000 rpm for 5 min at 4 °C to remove debris. The supernatants were then collected. The cellular uptake efficiency of the prepared rhodamine labeled LPs were determined by measuring the fluorescence intensity of rhodamine (excitation at 550 nm and emission at 590nm) using FP-750 Spectrofluorometer (JAS Co, Tokyo, Japan).

2.2.7. In vivo Biodistribution study

^{3}H-CHE labeled LPs and RLTR-PEG-LPs or KLGR-PEG-LPs were used to measure the biodistribution of liposomes in different organs in the mice. ICR mice were intravenously injected with ^{3}H-labeled LPs or RLTR-PEG-LPs. After 25 min, the animals were sacrificed; blood and other organs were collected and weighed. After weighing, the samples were solubilized in Soluene-350 (Perkin-Elmer Life Sciences, Japan) for overnight at 55 ^{0}C. Samples were decolorized by treatment with H_2O_2. The radioactivity of the samples was measured by using a liquid scintillation counting (*LSC-6100*, *Aloka, Japan*) after adding 10 ml of Hionic Flour (Perkin-Elmer Life Sciences, Japan) [81]. Tissue accumulation of LPs was represented as the percentage of injected dose (%ID) per organ.

2.2.8. Confocal microscopy experiment

ICR mice were given intravenous injection of Rhodamine labeled RLTR-PEG-LPs and the mice were killed 25 min after the treatment. The portal vein was cut and a needle was introduced into the vena cava and 10-15 ml of heparin containing PBS (40 units/ml) solution was used to remove the remaining blood and cell surface bound RLTR-PEG-LPs in the liver. The liver was then exscised and washed with saline and sliced into 10-15 mm-sized blocks with scissors. Then liver sections were then incubated with 20 fold volume of diluted solution of Hoechst 33342 (1mg/ml) and Isolectin B4 in HEPES buffer for 1 hr. The specimens were placed on a 35 mm glass base dish (IWAKI, Osaka, Japan) and observed by confocal laser scanning microscopy (A1 Confocal Laser Microscope System, Nikon Instruments Inc., Tokyo, Japan).

2.2.9. Inhibition assay

2.2.9.1 In vivo competitive inhibition study of RLTR-PEG-LPs

ICR mice were injected with unlabeled LPs and after 15 min, they were injected with cationic LP or RLTR modified PEG-LP or KLGR (reverse peptide sequence of RLTR) modified PEG-LP. After another 25 min of incubation the mice were sacrificed and the livers were perfused with 10 ml of a 40% heparin-PBS solution. The mice livers were then collected, sliced into 0.5mm x 0.5 mm pieces, stained with Hoechst 33342 and isolectin B4 and then observed by confocal microscopy (A1 Confocal Laser Microscope System, Nikon Instruments Inc., Tokyo, Japan).

2.2.9.2 In vitro competitive inhibition study of RLTR-PEG-LPs

40,000 LSECs were seeded in a 24-well plate and the plate was incubated overnight. After 24 hours, different concentrations of rhodamine labeled and unlabeled PEG-LPs (1:0, 1:5, 1:10, 1:20 and 1:50 respectively) were added and incubated for 3 hrs. After 3 hrs, the cells were washed 3 times with 1 ml of ice-cold phosphate buffer saline (PBS) which was supplemented with heparin (20 units/ml) to completely remove the surface-bound RLTR-PEG-LP and the intracellular fluorescence intensity of rhodamine was then determined [82]

.

2.2.10. Statistical analysis

Comparisons between multiple treatments were made using one-way analysis of variance (ANOVA), followed by the 'Dunnett test'. Pair-wise comparisons of subgroups were made using the student's t-test. Differences among the means were considered to be statistically significant at a p-value of <0.05 and <0.01.

2.3. Results

2.3.1. Synthesis of RLTR-PEG-DSPE

RLTR-PEG2000-DSPE was synthesized in accordance with the following scheme (fig. 2.2A). The thiol group of the cystein residue in the RLTR peptide was conjugated with Mal-PEG_{2000}-DSPE at 37°C for 24 hours. The synthesized RLTR-PEG-DSPE was confirmed by MALDI-TOF MS analyses. The peak corresponding to the molecular weight of RLTR-PEG-DSPE: MW 4368 (fig. 2.2 C) was consistent with the expected

product, i.e., conjugation between Maleimide-PEG-DSPE (calculated MW 2936 and observed MW 3109.24) (fig. 2.2B) and RLTR peptide (calculated MW 1441.68 and observed MW 1380).

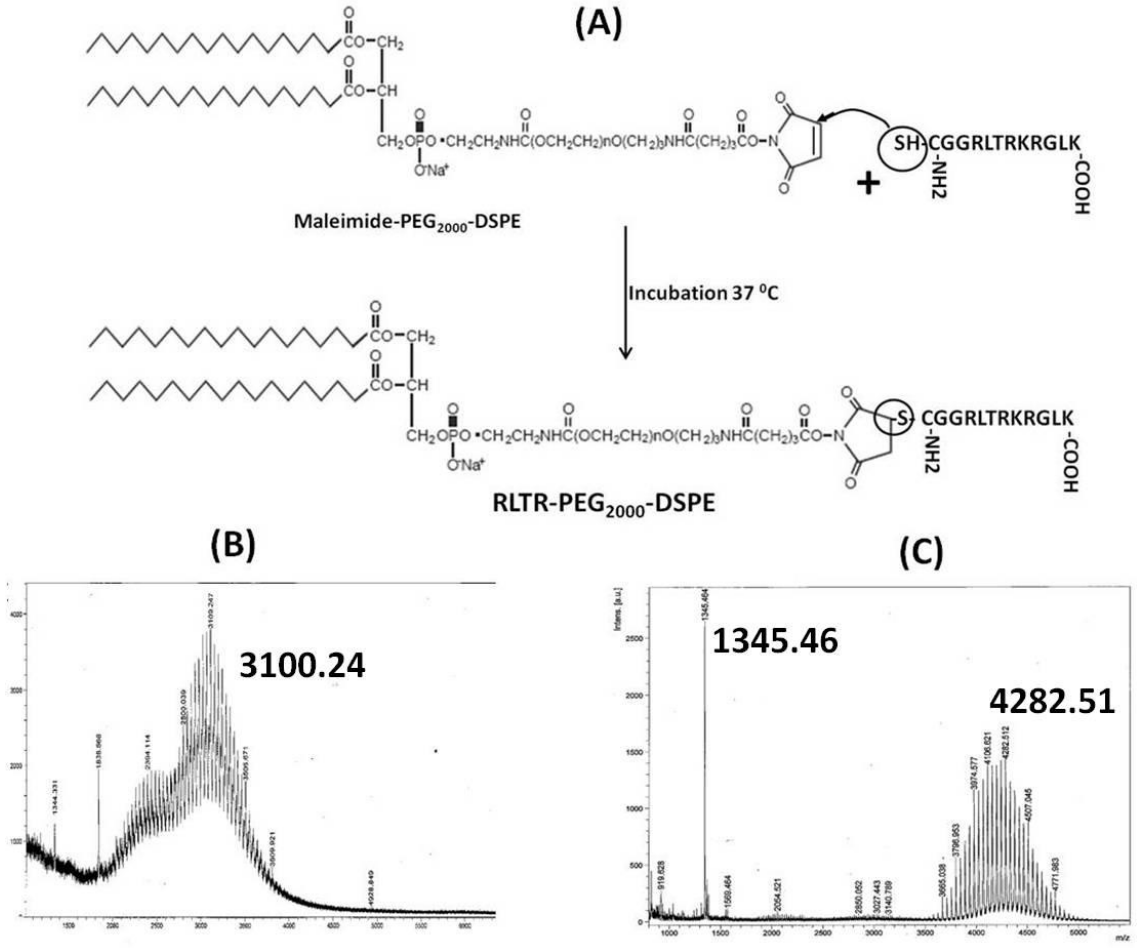

Figure 2.2. Conjugation of RLTR peptide with Maleimide-PEG2000-DSPE. (A) Synthesis of RLTR-PEG-DSPE by coupling of thiol group of the cysteine residue of RLTR peptide (calculated MW: 1343.7) with Maleimide-PEG_{2000}-DSPE (calculated MW: 2936). Maleimide-PEG_{2000}-DSPE and the RLTR peptide (molar ratio 1:1.2) were dissolved in water at 37 °C and allowed to react for 24 h. MALDI-TOF MS spectra of (B) Maleimide-PEG_{2000}-DSPE and (C) RLTR-PEG_{2000}-DSPE, which confirmed that the conjugation was successful, as evidenced by the molecular shifts of free RLTR peptide from 1343.9 (observed MW) to 4371.74 (observed MW) which is the sum of the individually calculated MW of RLTR peptide and Maleimide-PEG_{2000}-DSPE.

2.3.2. The characteristic of RLTR-PEG-LPs and its cellular uptake

The selected RLTR peptide was attached to the top of PEG in PEGylated liposomes. PEG liposomes (PEG-LPs) and RLTR modified PEG liposomes (RLTR-PEG-LPs) were prepared by incorporating PEG-DSPE or RLTR-PEG-DSPE at levels of 1, 3, 5, or 10 mol% of the total lipid. The physical properties of the prepared LPs are shown in Table 1. To evaluate the effect of the RLTR peptide on cellular uptake, we next examined the cellular uptake of RLTR-PEG-LPs and PEG-LPs in LSEC and in Hepa1-6 cell line. The RLTR peptide enhanced the cellular uptake of PEG-LPs and the maximum cellular uptake was observed within 3 mole% of RLTR peptide modification in both the cells (fig. 2.4A-B).

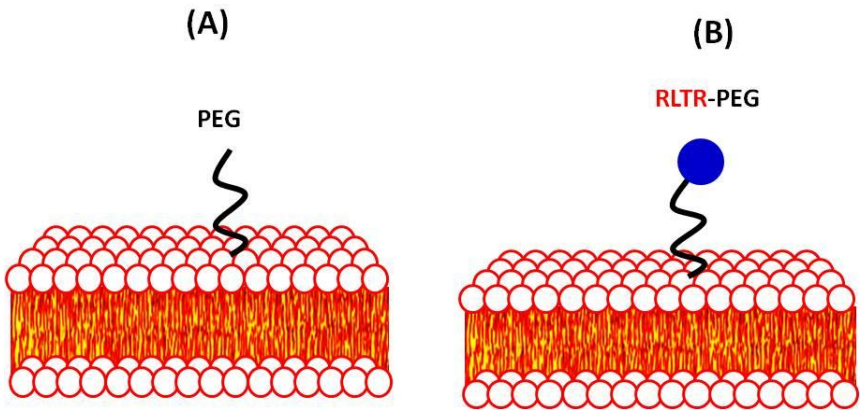

Figure 2.3. (A) PEG or (B)RLTR-PEG attached on the lipid bilayer of liposomes

Table 2.1: Physical properties of liposomes

% PEG-lipid	PEG-LP		RLTR-PEG-LP	
	Size (nm)	Zeta potential (mV)	Size (nm)	Zeta potential (mV)
0	92±10	-5±9		
1	102±8	-8±5	115±10	12±4
3	100±5	-20±8	121±14	20±6
5	105±7	-19±11	135±8	22±8
10	110±11	-24±12	132±10	27±3

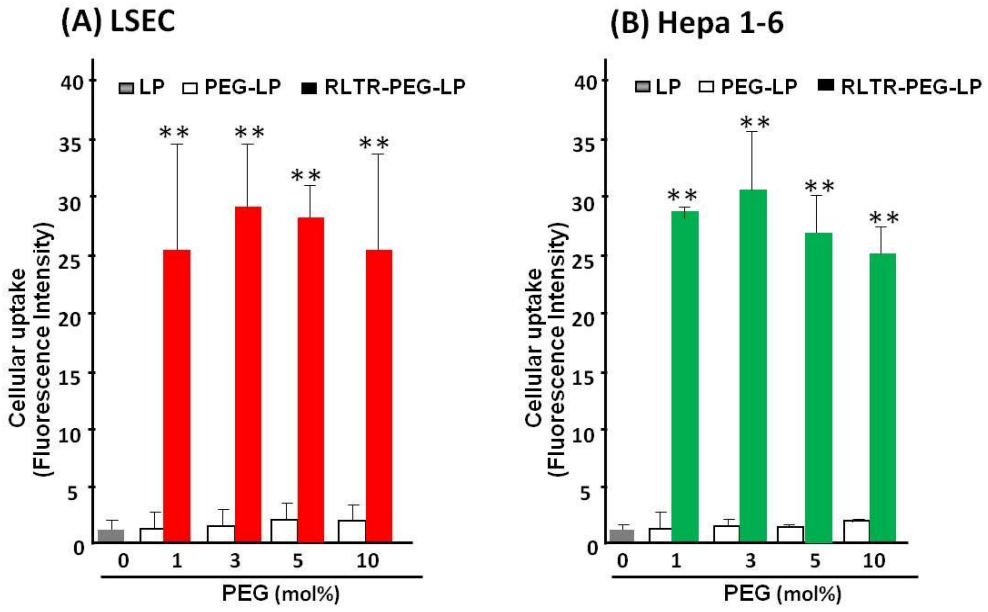

Figure 2.4 Cellular uptake of RLTR-PEG-LPs. For the cellular uptake study, 40,000 cells/well were seeded in a 24-well plate. After 24 hr LPs modified with different mol% of PEG-DSPE or RLTR-PEG-DSPE were incubated with (A) LSEC or (B) Hepa1-6 cells for 3 h and the cellular uptake efficiency of the prepared rhodamine labeled LPs were determined by measuring the fluorescence intensity of rhodamine. Cellular uptake is expressed as the mean ±SD (n=3) and Statistical analysis Vs LP was performed by One-way ANOVA followed by Dunnet-test. **P<0.01.

2.3.3. In vivo selectivity of RLTR peptide

A biodistribution study of RLTR-PEG-LPs was carried out in order to confirm the targeting ability of RLTR-PEG and KLGR-PEG-LP modified LP. Compared to unmodified control LPs, both the modified LPs were largely accumulated in the liver, with only negligible accumulation in the lung or spleen, within a very short time (fig. 2.5). The liver targeting ability of KLGR peptide was more than RLTR peptide and the difference was statistically significant. We then obtained an in vivo image of the liver to check the distribution pattern of this RLTR-PEG modified LP in liver.

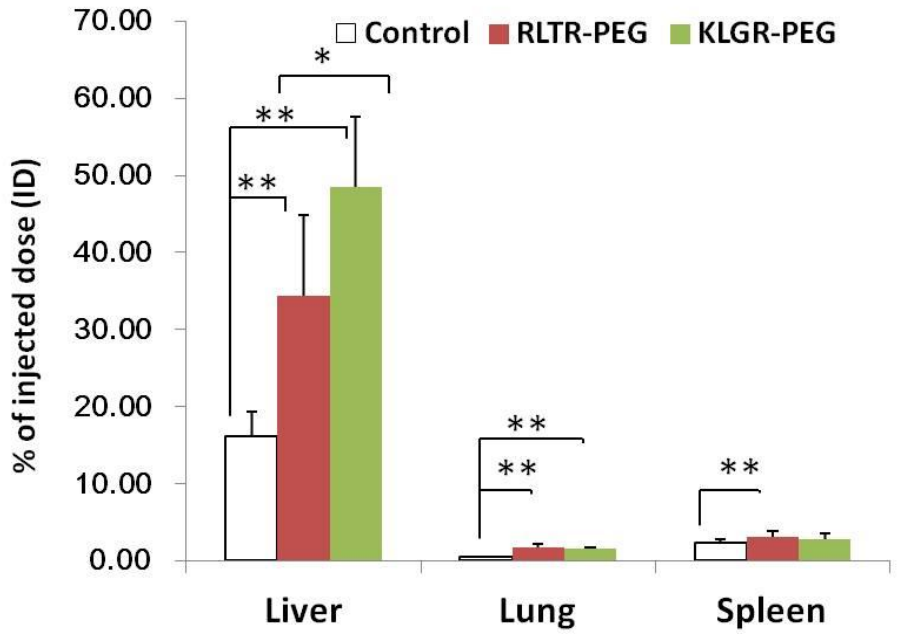

Figure 2.5. Biodistribution of 3H-CHE labeled RLTR-PEG-LPs, KLGR-PEG-LPs and LPs in different organ. Male ICR mice were intravenously injected with labeled RLTR-PEG-LPs, KLGR-PEG-LPs and LPs. After 25 min of incubation different organs of mouse were collected and radioactivity was measured. Tissue accumulation of LPs was represented as % of injected dose (ID). Here, % of ID is expressed as the mean ±SD (n=4). Statistical analysis is performed by unpaired Student's t-test, where *P<0.05, **P<0.01

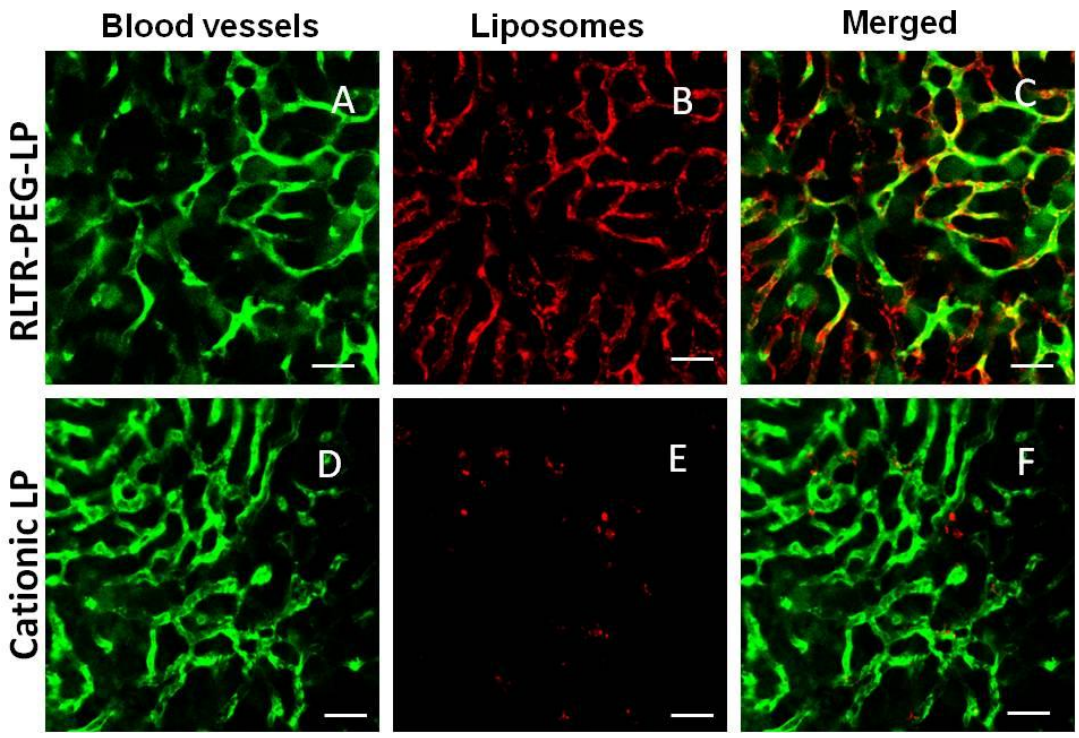

Figure 2.6. Representative intrahepatic distribution pattern of RLTR-PEG-LPs (A-C) and a cationic control LPs, in which the lipid composition was DC6-14/DOPE/Chol=4:3:3 (D-F). Green and red color represents blood vessels stained by Isolectin B4 and rhodamine labeled LPs respectively. Scale bars correspond to 50μm in all images.

We then performed an in vivo accumulation study to verify our hypothesis outlined in the introduction part. We investigated the intrahepatic distribution of RLTR-PEG-LPs by confocal microscopy. Rhodamine-labeled RLTR-PEG-LPs were widely distributed throughout the blood vessels (fig. 2.6B), and these intensities were essentially merged with the signal for Isolectin B4, a marker of endothelial cells (fig. 2.6C). These results demonstrate that RLTR-PEG-LPs efficiently target liver endothelial cells rather than hepatocytes. Furthermore, we compared the intrahepatic distribution pattern with RLTR-PEG-LPs and cationic LPs in order to evaluate the effect of the cationic charge of the liposomal surface. The size and zeta-potential of the Rhodamine-labeled RLTR-PEG-LPs and cationic LPs was 26mV, 125 nm and 22 mV, 132 nm respectively. The intrahepatic distribution pattern of the cationic LPs was quite different from that of the RLTR-PEG-LPs, in which the cationic LPs were gathered in particular spots (fig. 2.6E). In addition, these dots did not overlap with liver endothelial cells (fig.2.6F)

indicating that they were taken up by non-parenchymal cells such as kupffer cells or were merely aggregated LPs.

2.3.4. In vivo inhibition study

In order to examine some possible mechanisms of unique targeting ability of RLTR peptide into liver endothelial cells, comparative studies of RLTR and its reversed peptide sequence named as KLGR were performed in the following part. Both RLTR-PEG-LPs and KLGR-PEG-LPs were accumulated along with the liver blood vessels (fig. 2.7A-B, G-H). Next, accumulation of both labeled RLTR-PEG-LPs and KLGR-PEG-LP along with the liver blood vessels were dramatically inhibited by a pre-treatment with unlabeled RLTR-PEG-LPs or KLGR-PEG-LPs (fig. 2.7C-D, I-J), however, small portions of signal were remaining. In contrast, the accumulation of both eled RLTR-PEG-LPs or KLGR-PEG-LP was not reduced by the pre-treatment with unlabeled cationic LPs (fig. 2.7E-F, K-L). The results generated in this study suggest that cationic charge is not the reason for this uptake and may be both RLTR peptide and its reverse sequence, the KLGR peptide has some specificity for liver endothelial cells. Possible interpretations will be discussed in the discussion section.

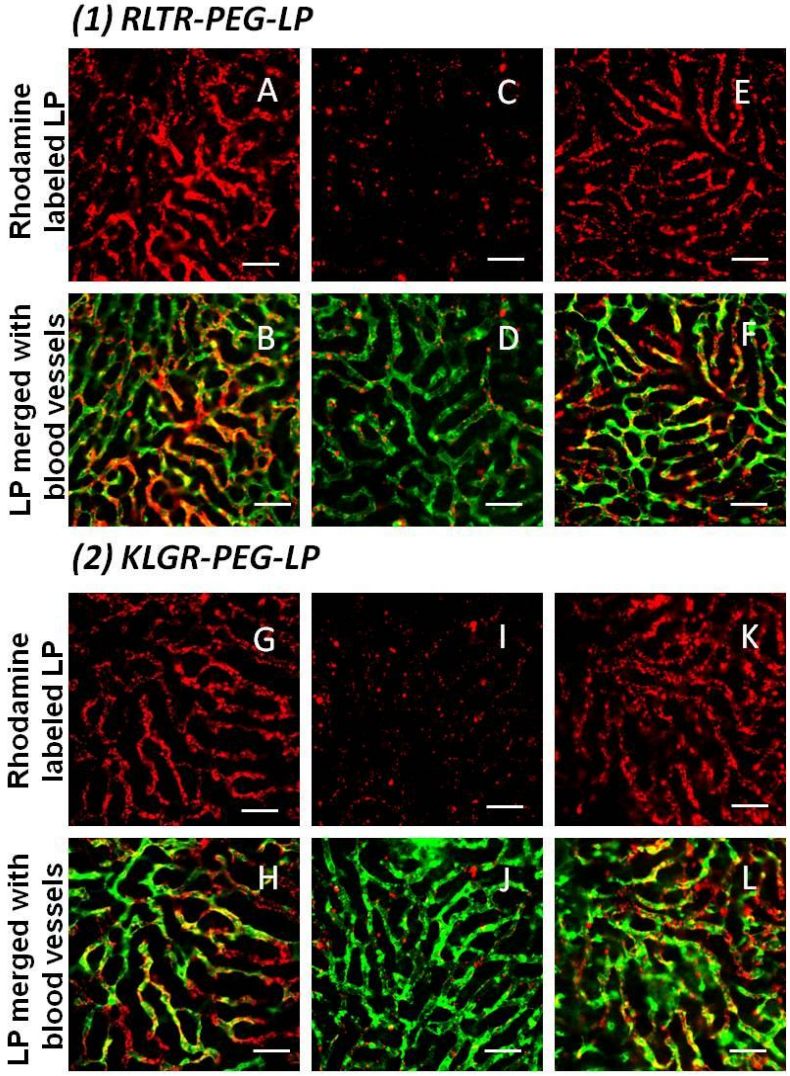

Figure 2.7. In vivo competitive inhibition studies of RLTR-PEG-LPs or KLGR-PEG-LPs using unlabeled RLTR-PEG-LPs or KLGR-PEG-LPs or cationic LPs. Green and red color represents blood vessels stained by Isolectin B4 and rhodamine labeled LPs respectively. Unlabeled RLTR-PEG-LPs or KLGR-PEG-LPs or cationic LPs were pre-treated with mice 15 minutes before the second treatment with labeled RLTR-PEG-LPs or KLGR-PEG-LPs for another 25 minutes of incubation. Representative images of liver tissues with (A, B) labeled RLTR-PEG-LPs, (C, D) labeled RLTR-PEG-LPs pre-treated with unlabeled RLTR-PEG-LPs, (E, F) labeled RLTR-PEG-LPs pre-treated with unlabeled cationic LPs, (G, H) labeled KLGR-PEG-LPs, (I, J) labeled KLGR-PEG-LPs pre-treated with unlabeled KLGR-PEG-LPs, (K, L) labeled KLGR-PEG-LPs pre-treated with unlabeled cationic LPs are shown. Scale bars correspond to 50μm in all images.

2.3.5. In vitro comparative inhibition study of RLTR-PEG-LPs

This experiment was performed to support the in vivo inhibition data. We compared the cellular uptake of both RLTR-PEG-LPs and KLGR-PEG-LPs with that of cationic-LPs under the inhibition with unlabeled RLTR-PEG-LPs or cationic-LPs. A comparative inhibition study with labeled and unlabeled LPs showed that the cellular uptake of labeled RLTR-PEG-LPs and KLGR-PEG-LPs were inhibited remarkably in the presence of a low amount of unlabeled RLTR-PEG-LPs and KLGR-PEG-LPs respectively (fig. 2.8A-B). On the other hand, the cellular uptake of labeled cationic LPs was not inhibited to a significant extent by unlabeled cationic LPs (fig. 2.8C). The results generated in this study suggest that both the RLTR and KLGR peptide efficiently delivered the nanocarriers into cells via a specific route, while cationic LPs were randomly taken up by cells. This conclusion is further supported by the in vivo comparative inhibition study.

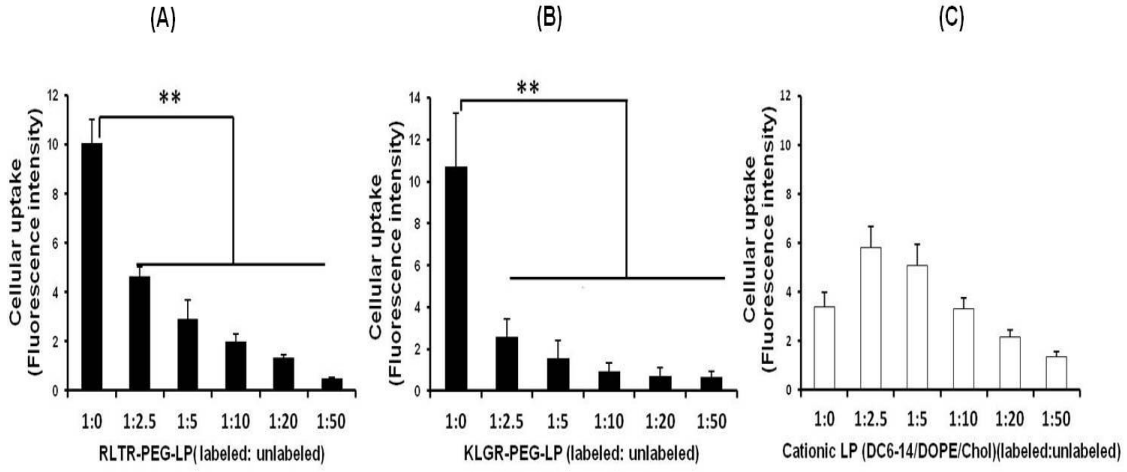

Figure 2.8. In vitro cellular uptake inhibition studies using unlabeled (A) RLTR-PEG-LPs, (B) KLGR-PEG-LP and (C) cationic LPs. Different ratios of labeled and unlabled LPs were co-incubated with 40,000 Liver ECs for 3 h. Data were expressed as the mean±SD (n=3) . Statistical differences vs. RLTR-PEG-LP (1:0) or KLGR-PEG-LP (1:0) or control LP (1:0) were determined by one-way ANOVA followed by Dunnett test. **P < 0.01.

2.4. Discussion

It has been reported that hepatocytes also express LDL receptors [74] and hepatocytes comprise 80% of the total liver volume [66]. In a recent study it was also demonstrated that LDL is taken up by LSECs [74]. In this present study we attempted to design a new ligand for hepatocytes based on the ApoB-100 sequence of LDL. The newly designed peptide ligand is referred to as RLTR. The size of the RLTR-PEG-LPs increased with the increase of the amount of RLTR-PEG. The surface charge of the PEG-LPs remained negative. However, the addition of the RLTR peptide resulted in a gradual increase in the surface charge of the PEG-LPs and a large difference in surface charge was observed between increments of RLTR-PEG of 1 mol% to 10 mol% (Table 2.1). This increment in surface charge of the RLTR-PEG-LPs reflects the cationic properties of the RLTR peptide. RLTR-PEG-LPs showed a remarkable enhancement in cellular uptake compared to PEG-LPs in different cell types including LSEC and Hepa 1-6 cell lines (fig. 2.4 A-B). In the biodistribution study it was also observed that most of the RLTR or KLGR modified PEG-LP has been accumulated in liver rather than other organs like lung or spleen (fig. 2.5). However, in confocal microscopy images it was observed that, RLTR-PEG-LPs accumulated at high levels in liver blood vessels (fig. 2.6 A-C) which indicate that these liposomes do not accumulate in hepatocytes. The cellular accumulation of RLTR-PEG-LPs was significantly higher than that of cationic LPs (fig. 2.7D-F). Though the RLTR peptide is designed from LDL and there is previous report that LDL is rapidly taken up by LDL receptors, the peptide modified PEG-LP is highly accumulated in LSEC. It is possible that this carrier system has more specificity for LSEC, rather than hepatocytes. This surprising accumulation of this carrier system through blood vessels caused us to conclude that this nanoparticle might be an ideal system for targeting the liver endothelial cells. The fact that cationic peptides and lipids accumulate at high levels in endothelial cells of liver is attractive. There are very few reports of targeting liver endothelial cells using cationic or neutral nano carriers [84, 85]. It should be noted that, these systems failed to achieve high accumulation in liver endothelial cells. Because of this, in this study we seized the opportunity to develop this nanocarier to target LSEC. There are two possible reasons for the high accumulation of RLTR modified PEG-LP in LSEC. Either the high cationic charge of the peptide is causing this high accumulation or the peptide sequence itself has specificity for liver

endothelial cell. We then checked the specificity of both RLTR and its reverse sequence KLGR modified PEG-LP by both an in vitro and in vivo inhibition study. In the in vivo inhibition study we demonstrated that both the RLTR-PEG-LPs and KLGR-PEG-LPs uptake were inhibited by unlabeled RLTR-PEG-LPs and KLGR-PEG-LPs respectively (fig. 2.7). However, the cationic LPs did not affect its uptake both in vivo or in vitro (fig. 2.7 and 2.8). Given these findings, the possibility of a higher accumulation in LSEC is due to a higher cationic charge can be excluded. We then attempted to address the second possible reason of the higher accumulation in LSEC, which is the sequence of the peptide. We found that the sequence contain a motif RKR which remains the same both in the RLTR and KLGR peptide, although the sequence is completely reversed. It has been reported that stearylated polyarginine and its derivatives, i.e. stearyl-$(RXR)_4$ mediates the efficient plasmid transfection in several cell lines [86]. The RKR motif is similar as the RXR motif (fig. 2.9). As our study shows that both the RLTR (RLT**RKR**GLK) and KLGR (KLG**RKR**TLR) modified PEG-LP are equally efficient in targeting LSEC, the possibility that the RKR sequence is responsible for this targeting cannot be completely excluded. There is another possibility, i.e. both peptides contains an RXXR motif. According to CendR theory this RXXR sequence is essential for a tissue penetrating property [87]. As our peptide sequence RLTR (**RLTR**KRGLK) and KLGR (**KLGR**KRTLR) both have the RXXR sequence and supporting CendR theory so there is another possibility that **RLTR** and **KLGR** are the true motifs for these two peptides for targeting LSEC (fig. 6). Both the peptide, RLTR and KTLR, modified LPs appear to have similar targeting abilities for LSEC. However, we were not able to identify the receptor or the key motif responsible for this targeting. Further study will be required to identify the motif or the receptor. LDL receptor, LRP-1, RXR or RXXR motif, which are mentioned in the introduction and discussion, are all possibilities.

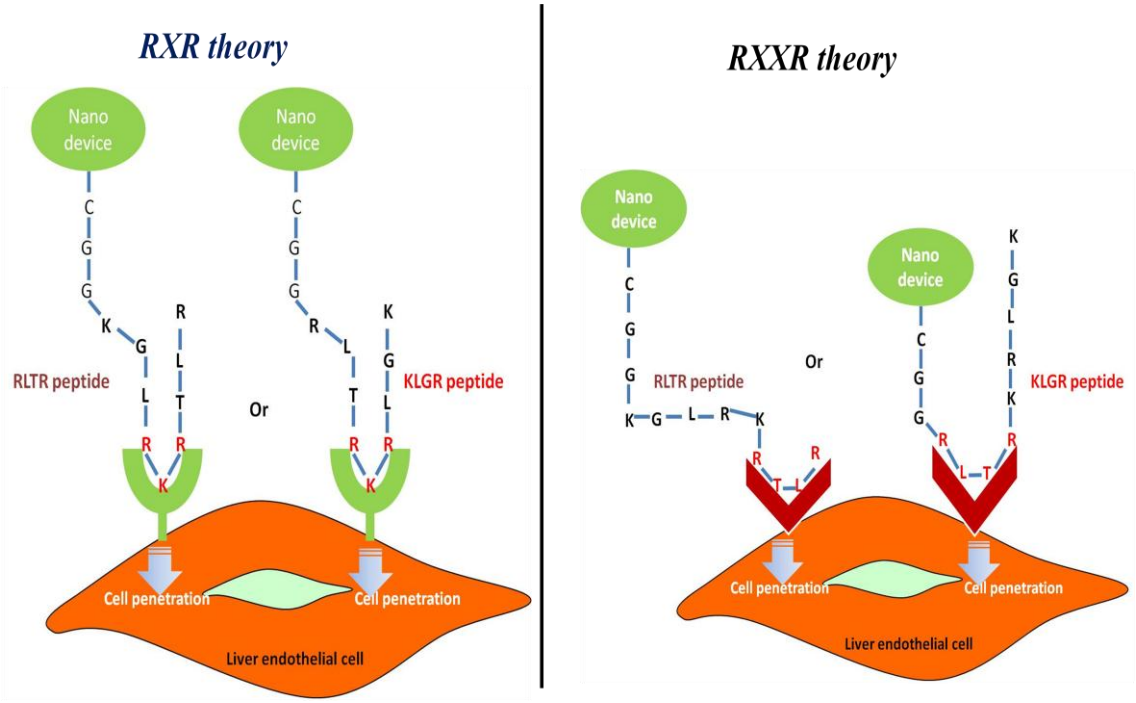

Figure 2.9. Proposed theory for similar binding and cell penetration of RLTR and KLGR (reverse sequence of RLTR peptide) modified PEG-LPs. Where (A) shows binding of the RXR motif in both the peptide modified LPs with the receptor expressed by LEC and (B) shows binding of RXXR (RXXR represents either RLTR or RTLR motif) of RLTR or KLGR modified LPs respectively to the receptor expressed by LSEC.

2.5. Conclusion

Liposomes modified with the peptide sequence RLTRKRGLK or its reverse sequence KLGRKRTLR, designed based on the ApoB-100 sequence, accumulated at high levels in liver endothelial cells via some as-yet-unidentified target receptors, and not via non-specific binding with the cell surface. The RLTR or KLGR modified liposomes have the potential for use as a carrier system for the delivery of drugs to liver endothelial cells.

3

Formulation of new peptide-conjugated MEND and delivering siRNA to LSEC

3.1. Introduction

LSECs are located at the liver sinusoids where they separate hepatocytes from blood flow. They play important role in normal physiological conditions as well as in many pathophysiological situations [9, 10]. Upon exposure to any chemical toxins or any viral infection or due to stimulation by cytokines or chemokines they undergo into a huge change in gene expression and thus actively took part in inflammatory conditions [33, 45-47].

Disturbances of normal LSEC functions contribute to a wide range of pathophysiology. For example, altered microcirculation due to change in the porosity of LSEC has been implicated in alcoholic liver disease [88]. Despite of initiating different hepatic disease LSEC induces disease progression by playing active role in terms of immunity and inflammation [45]. To normalize the altered physiology or to reduce the induction of inflammation during various pathophysiological condition gene delivery to LSEC can become an useful therapeutic agent. But currently this approach is not successful because of lack of a specific carrier. However, in this study we tried to develop a targeted naocarrier specific to LSEC.

In the area of gene delivery, siRNA delivery has been proved to be advantageous in terms of efficacy. One of the main obstacles for this therapy is specificity. In this study, multifunctional type nano device or MEND was used as siRNA carrier. For this purpose we used previously reported YSK05-MEND which was reported to show successful RNAi activity in liver [89].

To increase the specificity of the MEND we decided to modify the MEND surface with an LSEC selective ligand. For this purpose previously reported KLGR peptide (chapter 2) was used. This peptide ligand was designed from ApoB-100 sequence of LDL molecule which is responsible for the binding of LDL molecule to LDL receptor [53, 54]. Stearylated KLGR (STR-KLGR) modified YSK05-MEND was able to deliver Tie2 siRNA into LSEC to suppress the endothelial cell specific Tie2 gene which is also known as angiopoietin receptor protein. Tie2 siRNA delivery to liver caused significant decrease in the expression of tie2 gene which establishes selectivity of the STR-KLGR modified YSK05-MEND to LSEC. Here, in this study, we made additional effort not only to prove selectivity of the carrier to LSEC rather than hepatocytes but also optimized the carrier to achieve maximum gene silencing activity.

3.2. Materials and methods

3.2.1. Materials

We purchased F7 siRNA (sense strand): 5'-GGAUCAUCUCAAGUCUUACdTdT-3' and Tie2 siRNA (sense strand): 5'-AUAUCUGGGCAAAUGAUGG-3' from Sigma (Ishikari, Japan). RLTRKRGLKGGC (KLGR in brief) peptide and Stearylated RLTRKRGLK (STR-KLGR) and stearylated octaarginine (STR-R8) peptides were purchased from Kurabo Industries, Osaka, Japan. 1,2-dimyristoyl-sn-glycerol, methoxyethyleneglycol 2000 ether (PEG-DMG), Cholesterol (Chol) were purchased from Avanti Polar Lipids (Alabaster, AL, USA). N-[(3-maleimide-1-oxopropyl) aminopropyl polyethyleneglycol-carbamyl] distearoylphosphatidyl-ethanolamine (maleimide-PEG-DSPE) was purchased from Nippon Oil and Fat Co. (Tokyo, Japan). Endothelial Cell Basal Medium (EBM-2) and other related growth factors were purchased from Lonza (Walkersville, MD, USA). Fetal bovine serum (FBS) was obtained from Hyclone Laboratories (Logan, UT, USA). Ribogreen was purchased from Molecular Probes (Eugene, OR, USA). TRIZOL reagents were purchased from Invitrogen (Carlsbad, CA, USA). All other chemicals used in this study were of analytical grade.

3.2.2. Experimental animals

Male ICR mice were purchased from Japan SLC (Shizuoka, Japan). The experimental protocols were reviewed and approved by the Hokkaido University Animal Care Committee in accordance with the guidelines for the care and use of laboratory animals.

3.2.3. Cell culture

Hepa1-6 cells were obtained from the American Type Culture Collection (Manassas, VA) and the cells were maintained with Dulbecco's modified Eagle's medium (DMEM) supplemented with 10% fetal bovine serum and penicillin (100 units/ml) under an atmosphere of 5% CO2 at 37 °C. Liver Sinusoidal Endothelial cell (LSEC) were maintained in Endothelial Cell Basal Medium (EBM-2) supplemented with 2% FBS (v/v), penicillin (100 units/ml), streptomycin (100 mg/ml) and other relevant growth factors. The cells were cultured under an atmosphere of 5% CO2 at 37 °C.

3.2.4. Conjugation of the KLGR peptide to PEG_{2000}-DSPE

Conjugation was achieved by incubating a 1.2:1 molar ratio of RLTRKRGLKGGC peptide and maleimide-PEG-DSPE in deionized water at room temperature for 24 hrs. The conjugation of KLGR with PEG was confirmed by matrix assisted laser desorption/ionization-time of flight (MALDI-TOF) MS (Bruker Daltonics, Germany) using acetonitrile: water=7:3 with 0.1 % of trifluoroacetate as the matrix solution, supplied with a 10 mg/ml solution of dihydroxybenzoic acid.

3.2.5. Preparation of MEND

We used YSK05-MEND in this experimental works. This MEND was developed by our laboratory previously [89]. The same protocol as reported before was followed to prepare MEND. t-BuOH dilution procedure was followed to prepare this MEND. The MENDs component was YSK05/cholesterol/PEG-DMG at a molar ratio of 30/40/30/3. Empty MEND with the same lipid composition was prepared by a similar procedure, with an exception that an equivalent volume of 1 mM citrate buffer was titrated to the lipid solution instead of siRNA complex. For modifying the MEND surface with KLGR-PEG or STR-KLGR, the MENDs were incubated at 45 °C for 45 min with KLGR-PEG or STR-KLGR. Labeled MENDs were prepared by adding 1 mol% of NBD-DOPE to the

lipid-t-BuOH solution prior to mixing with the siRNA. The average size and zetapotential of MENDs were measured by a Zetasizer Nano ZS ZEN3600 (Malvern Instruments, Worcestershire, UK).

3.2.6. Ribogreen assay

For the determination of siRNA encapsulation efficiency of developed MEND and to measure concentration of siRNA, Ribogreen fluorescence assay was performed [90]. RiboGreen (Molecular Probes, OR, U.S.A.) that binds specifically to double-stranded siRNA and gives fluorescence intensity only when bound with siRNA. Fluorescence intensity was measured with a spectrofluorometer (Enspire 2300 multilabel Reader, Perkinelmer) using excitation and emission wavelengths of 495 and 525 nm. First MENDs were diluted differently in 10 mM HEPES buffer at pH 7.4. Then Ribogreen was added to all the samples at a 1:1 ratio (v/v) either in the presence or absence of 0.1% (w/v) Triton X-100. A standard curve was prepared using different concentration of siRNA and the siRNA concentration in MEND was calculated from siRNA standard curve. siRNA encapsulation efficiency was measured by comparing siRNA concentration in the presence and absence of Triton X-100.

3.2.7. In vivo gene delivery study

For measurement of Knockdown efficiency of Tie2 or FVII gene expression by YSK05-MEND modified with different mol% of KLGR-PEG or STR-KLGR or STR-R8, the male ICR mice were injected intravenously with either Tie2 siRNA or FVII siRNA encapsulated modified or unmodified YSK05-MEND at an siRNA dose of 1 mg/kg of body weight. After 24 hr of incubation the mice were sacrificed and livers, lung or kidneys were collected.

3.2.8. RNA extraction and PCR analysis

RNA was extracted from mouse tissues (liver, lung and kidney) using TRIzol Reagent (Invitrogen Inc.). cDNA was prepared from 1 µg of RNA using the High Capacity RNA-to-cDNA Kit (ABI), according to the manufacturer's instructions. The resulting cDNA was diluted, and a 5 µl aliquot was used in a 20 µl PCR reaction (SYBR Green; TOYOBO) containing specific primer sets at a concentration of 250 nM each. PCR

reactions were run in duplicate and quantified using the Mx3005P Real-time QPCR system (Agilent). Cycle threshold (Ct) values were normalized to beta-actin expression, and results were expressed as the fold change in mRNA compared with control mice.

3.2.9. Confocal microscopy experiment

ICR mice were given intravenous injection of rhodamine labeled STR-KLGR modified MEND and the mice were killed 25 min after the treatment. The portal vein was cut and a needle was introduced into the vena cava and 10-15 ml of heparin containing PBS (40 units/ml) solution was used to remove the remaining blood and cell surface bound MEND in the liver. The liver was then excised and washed with saline and sliced into 10-15 mm-sized blocks with scissors. Liver sections were then incubated with 20 fold volume of diluted solution of Hoechst 33342 (1mg/ml) and Isolectin B4 in HEPES buffer for 1 hr. The specimens were placed on a 35 mm glass base dish (IWAKI, Osaka, Japan) and observed by confocal laser scanning microscopy (A1 Confocal Laser Microscope System, Nikon Instruments Inc., Tokyo, Japan).

3.2.10. In vitro quantitative cellular uptake study

The quantitative measurement of cellular uptake of the STR-KLGR modified MEND was determined by flow cytometry. Empty MENDs modified with or without STR-KLGR at different mol% were prepared as described above. MENDs were labeled with NBD-DOPE. Primary LSECs were seeded at a density of 200000 cells per well in a 6-well plate with medium. After 24 h of seeding period, the cells were incubated with MENDs in serum free medium for 1 h. The cells were then washed with PBS (-) supplemented with heparin solution (20 unit/mL). Then trypsin was added to each well and every sample was collected in different eppendorf tube by centrifugation (3000 rpm, 4 degree C, for 3 min). Cell pellets were resuspended in 1 mL of PBS (-) supplemented with 0.5% BSA and 0.1% NaN_3 (FACS buffer). Then the cells were filtered through a nylon mesh to remove aggregated cell and debries. The filtered cells were analyzed by flow cytometry (FACScan, Becton Dickinson). The cellular uptake of NBD-DOPE labeled MEND was expressed as the mean fluorescence intensity, calculated using the CellQuest software (Becton Dickinson).

3.2.11. Endosomal escape efficiency of STR-KLGR modified MEND

100000 LSECs were seeded on a 35-mm glass-base dish (Iwaki, Chiba Japan) in 2 ml of EBM-2 medium containing serum and other essential factors. After 24 hr of seeding the culture medium was removed and the cells were washed with 1 ml of serum-free medium. Then the cells were incubated with cy3 labeled siRNA loaded MEND either modified or unmodified with STR-KLGR. Then after 30 minutes of incubation at 37 degree C, Lysotracker green was added to the cell dish to stain endosomal/lysosomal compartment. Then after 45 minutes of incubation Hoechst 33342 was added to stain cell nucleus. Then after total 1 hr of incubation medium was washed with PBS supplemented with heparin (20 units/mL) for 3 times. Then the cells were kept in Kreb's buffer and confocal images were taken by confocal laser scanning microscopy (A1 Confocal Laser Microscope System, Nikon Instruments Inc., Tokyo, Japan). Minimum 6-8 pictures were taken where there was minimum 2-3 cells in each image with CFI Apochromat TIRF 60x oil, NA1.49 lense. Then each image was transferred to Scope-Pro 7.0 configuration software to quantify the pixel areas in each cell separately. For every sample total 10 cells were analyzed. Then the endosomal escape efficiency for every particular cell was calculated as follows:

Percentage of endosomal escape=
[Total area of siRNA (both in lysosme/endosome and in the cytosol)-Total area of siRNA (in endosome/Lysosome)]/ Total area of siRNA (both in lysosme/endosome and in the cytosol) X 100

3.2.12. Uptake mechanism study

For the investigation of mechanism of cellular uptake of STR-KLGR modified MEND 200000 primary LSECs or Hepa 1-6 cells were seeded on a 35-mm glass-base dish (Iwaki, Chiba, Japan) in 2 ml of EBM-2medium supplemented with serum and other essential factorsfor 24 h. At the day of experiment the cells were washed with 1 ml PBS. Then the dishes were pre-incubated with serum-free medium in the absence or presence of inhibitor. The following inhibitors were added separately in separate dishes and incubated for different time schedule: amiloride (5 mM) for 30 min, filipin (150 μg/ml) for 45 min and sucrose (0.5 M) for 30 min. Then after the mentioned incubation time

50nM of STR-KLGR modified or unmodified MEND encapsulating cy3 labeled Tie2 siRNA was added and the cells were incubated with or without inhibitor for another 1 hr. Nuclei were stained with Hoechst 33342 for 10 min before washing. The cells were then washed with 1 ml of ice-cold phosphate buffer saline (PBS) supplemented with heparin (20 units/ ml) for three times to completely wash the surface bound MEND. The cells then were kept on ice in 2ml of Krebs buffer and images were taken by confocal microscopy.

3.2.13. Toxicological study

For toxicological studies 4wk male ICR mouse were injected intravenously with STR-KLGR modified YSK05-MEND encapsulating Tie2 siRNA at a siRNA dose of 1 mg/kg body weight. After 24 hour of incubation blood samples were collected by syringe from heart and then serum levels of aspartate aminotransferase (AST) and alanine aminotransferase (ALT) were measured using a colorimetric diagnostic kit (Wako Pure Chemical Industries Ltd.) according to the manufacturers guide.

3.2.14. Statistical analysis

Statistical significance of multiple treatments were calculated using one-way analysis of variance (ANOVA), followed by 'Dunnett test'. Pair-wise comparisons of subgroups were made using the student's t-test. Differences among the means were considered to be statistically significant at a p-value of <0.05 and <0.01.

3.3. Results

3.3. 1. Synthesis of KLGR-PEG-DSPE

KLGR-PEG_{2000}-DSPE was synthesized in accordance with the following scheme (fig. 3.1A). The thiol group of the cystein residue in the KLGR peptide was conjugated with Mal-PEG_{2000}-DSPE at 37°C for 24 hours. The synthesized KLGR-PEG-DSPE was confirmed by MALDI-TOF MS analyses. The peak corresponding to the molecular weight of KLGR-PEG-DSPE: MW 4282.5 (observed MW: 4271 (fig. 3.1C) was consistent with the expected product, i.e., conjugation between Maleimide-PEG-DSPE (calculated MW 2936 and observed MW 3109.24) (fig. 3.1C) and KLGR peptide (calculated MW 1340 and observed MW 1345.4).

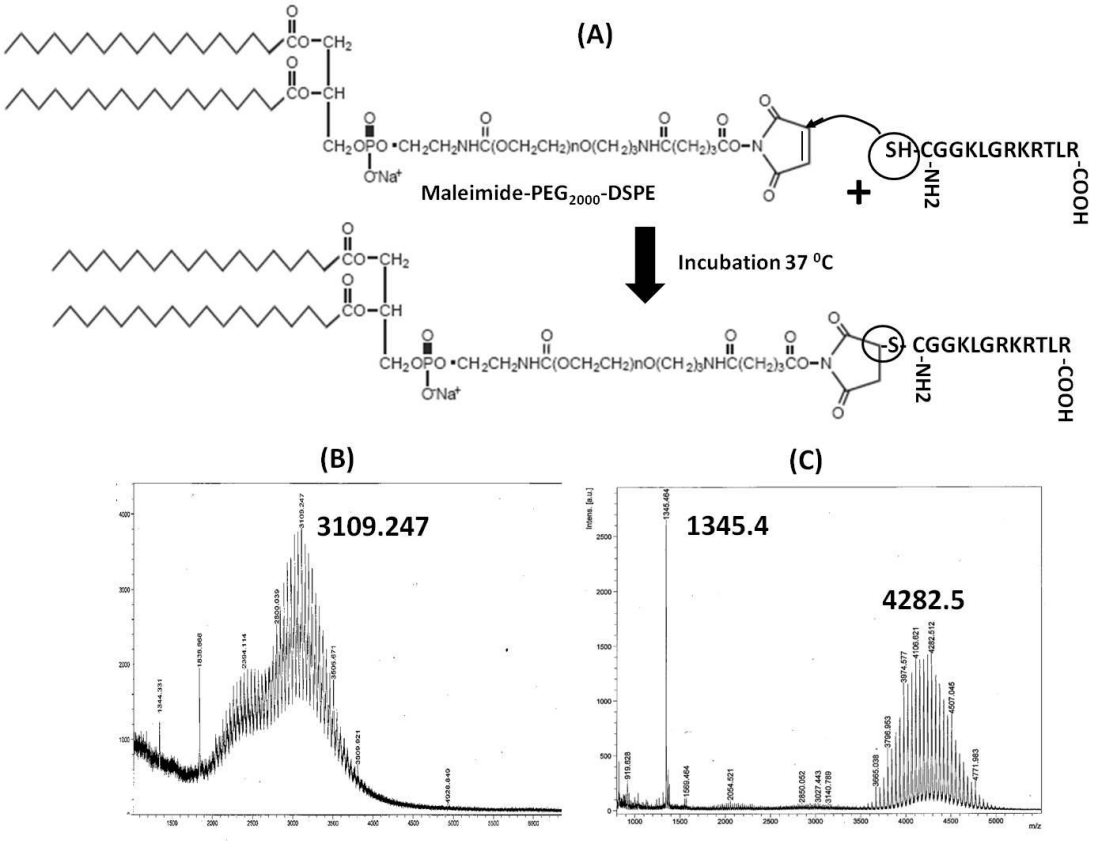

Figure 3.1: Conjugation of KLGR peptide with Maleimide-PEG$_{2000}$-DSPE. (A) Synthesis of KLGR-PEG$_{2000}$-DSPE by coupling of thiol group of the cysteine residue of KLGR peptide (calculated MW: 1340) with Maleimide-PEG$_{2000}$-DSPE (calculated MW: 2936). Maleimide-PEG$_{2000}$-DSPE and the KLGR peptide (molar ratio 1:1.2) were dissolved in water at 37 °C and allowed to react for 24 h. MALDI-TOF MS spectra of (B) Maleimide-PEG$_{2000}$-DSPE and (C) KLGR-PEG$_{2000}$-DSPE, which confirmed that the conjugation was successful, as evidenced by the molecular shifts of free KLGR peptide from 1345.4 (observed MW) to 4282.5 (observed MW) which is the sum of the individually calculated MW of KLGR peptide and Maleimide-PEG$_{2000}$-DSPE.

3.3.2. The characteristic of KLGR-PEG or STR-KLGR modified YSK05 MEND

The YSK05-MEND was modified with different mol% of KLGR-PEG or STR-KLGR. The physical properties of the prepared MENDs are shown in Table 4.1. Particle size of MEND and zeta-potential were measured by Malvern Zetasizer. Average diameter of YSK05-MEND was within the range of 80 to 120 nm. Addition of ligand at the MEND surface did not affect the size much until 5 mol% STR-KLGR at the surface of MEND.

The surface charge of unmodified YSK05-MEND was almost neutral (6 mV), while addition of ligand increased the surface charge with the increase of ligand density at the MEND surface. The surface charge of YSK05-MEND was within the range of 8 to 25 mV. Percentage of siRNA encapsulation was measured by ribogreen assay which showed that in every experiment the siRNA encapsulation efficiency ranges from 75 to 90%.

Table 3.1: Physical characteristics of YSK05-MEND

Sample	KLGR-PEG$_{2000}$-YSK05-MEND		Str-KLGR-YSK05-MEND	
	Size (nm)	Zeta potential (mV)	Size (nm)	Zeta potential (mV)
YSK05-MEND$_{0\%\ KLGR}$	84	6		
YSK05-MEND$_{1\%\ KLGR}$	86	12	90	8
YSK05-MEND$_{3\%\ KLGR}$	84	18	81	19
YSK05-MEND$_{5\%\ KLGR}$	118	22	103	25

3.3.3. In vivo gene silencing activity of KLGR-PEG or STR-KLGR modified YSK05 MEND

An in vivo gene expression knockdown experiment was performed to evaluate the siRNA delivery capacity of our developed carrier to LSEC. For the measurement of knockdown efficiency of expression of Tie2 gene, an endothelial cell specific marker, Tie2 siRNA was delivered through KLGR-PEG or STR-KLGR modified YSK05-MEND. In fig. 3.2 it is shown that KLGR-PEG modified YSK05-MEND failed to show significant knocking down of gene expression while in case of STR-KLGR maximum knockdown of Tie2 gene was observed at 1 mol% of ligand density at the MEND surface. And the gene expression was increased with the increase of mol% of STR-KLGR at the MEND surface. From the data it is clear that though amount of ligand for the modification of surface of MEND was increased but the knockdown of gene expression was decreased.

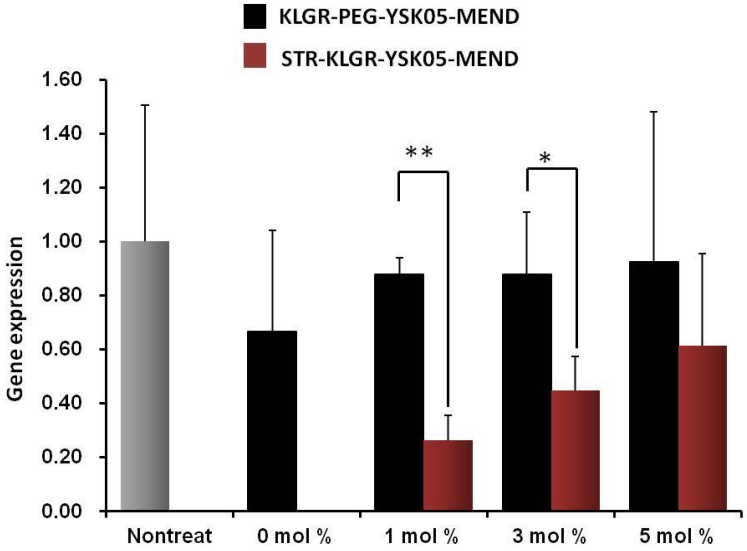

Figure 3.2: In vivo Tie2 gene expression by YSK05-MEND modified with different mol% of KLGR-PEG or STR-KLGR. Male ICR mice were intravenously injected with YSK05-MEND modified with different mol% of KLGR-PEG or STR-KLGR encapsulating Tie2 siRNA in the core. After 24 hr of incubation liver samples were collected. After collecting mRNA from liver samples Tie2 gene expression level was measured by RT-PCR Number of mouse in each sample group=6, Statistical analysis within each groups was done by unpaired t-test, where **P<0.01 and*P<0.05

3.3.4. In vivo accumulation of STR-KLGR modified YSK05-MEND in liver

As in the previous section we find that the knockdown effect of gene expression did not increased with the increased mol% of ligand at the surface of YSK05-MEND we took an attempt to perform an *in vivo* accumulation study of the developed nano carrier to liver by confocal microscope. The accumulation pattern of STR-KLGR modified YSK05-MEND shows that the uptake of modified MEND increases with the increase of ligand density at the surface of MEND (fig. 3.3). The rhodamin-DOPE labeled YSK05 MEND merges with isolectin B4 stained blood vessels, which pointing to the accumulation of MEND through the blood vessels.

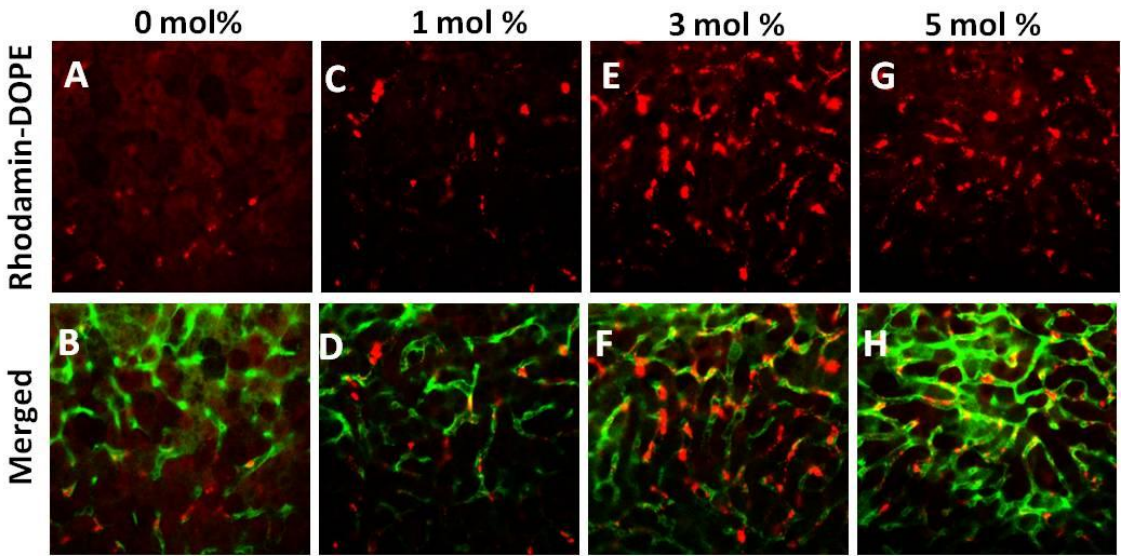

Figure 3.3: In vivo accumulation of YSK05-MEND modified with 0 mol% (A-B), 1 mol% (C-D), 3 mol% (E-F) and 5 mol% (G-H) of STR-KLGR. Green and red color represents blood vessels stained by Isolectin B4 and rhodamine labeled MEND respectively.

3.3.5. Cellular uptake by flow cytometry

To support the *in vivo* uptake result of YSK05-MEND modified with different mol% of STR-KLGR we performed an *in vitro* quantitave uptake measurement by flow cytometry. In this experiment (fig. 3.4) the cellular uptake of STR-KLGR modified YSK05-MEND in LSEC increases with an increase in the amount of STR-KLGR at the YSK05-MEND. There is complete shift in fluorescence intensity with the increase in modification rate of MEND (fig. 3.4A). When the cellular uptake in terms of mean fluorescence intensity was plotted the graph shows a gradual increase in the cellular uptake with increase in ligand at the surface of MEND (fig. 3.4B). This data completely supports the in vivo result. Comparing the cellularaccumulation and gene expression data (fig. 3.2 and 3.3) it seems that knockdown of gene expression is maximum when the surface modification of YSK05-MEND by STR-KLGR is minimum, for e.g. 1 mol%. So we decided to check the knockdown efficiency of YSK05-MEND when the ligand density at the MEND surface is lower than 1 mol%.

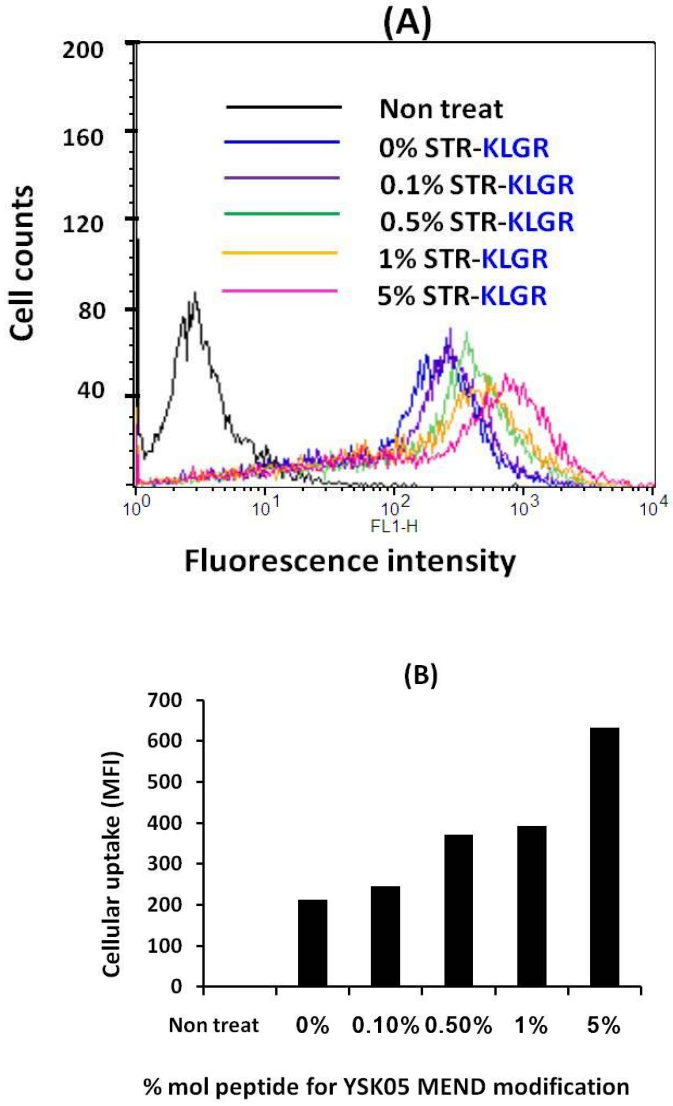

Figure 3.4: In vitro cellular uptake study by flow cytometry. (A) Fluorescence intensity of NBD-DOPE labeled YSK05-MEND modified with different mol% of STR-KLGR and (B) Mean fluorescence intensity (MFI) of STR-KLGR modified NBD-DOPE labeled YSK05-MEND taken up by LSECs.

3.3.6. Effect of low density of STR-KLGR at YSK05-MEND in *in vivo* gene expression

We performed this study to compare the effect of low amount of STR-KLGR with high amount of STR-KLGR at the YSK05-MEND surface. In this study we considered 1 mol% of STR-KLGR as high density of ligand as it showed maximum knock down effect of Tie2 gene expression (fig. 3.5). As low density of ligand we compared 0.1 mol% and 0.5

mol% of STR-KLGR. As KLGR is a highly cationic peptide we also compared STR-KLGR modified YSK05-MEND with STR-R8 modified YSK05-MEND. The data showed that 0.5 mol% of STR-KLGR modified YSK05-MEND showed better knocking down of Tie2 gene expression than 1 mol% STR-KLGR modified YSK05-MEND (fig. 3.5). It also showed better knockdown efficiency than STR-R8 modified YSK05-MEND.

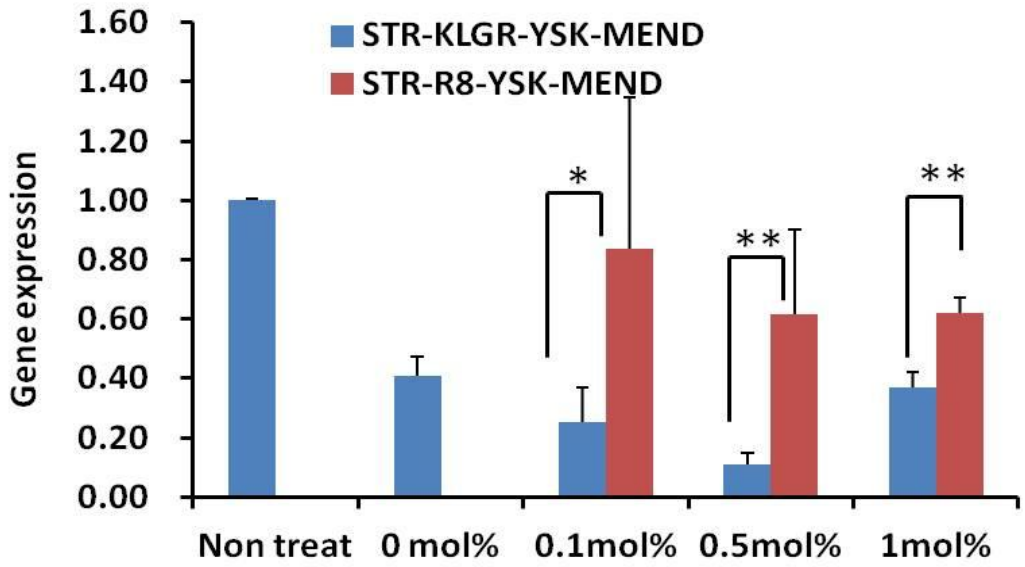

Figure 3.5: In vivo Tie2 gene expression by YSK05-MEND modified with low density of STR-KLGR or STR-R8 at the MEND surface. Male ICR mice were intravenously injected with YSK05-MEND modified with different mol% of STR-KLGR or STR-R8 encapsulating Tie2 siRNA in the core. After 24 hr of incubation liver samples were collected. After collecting mRNA from liver samples Tie2 gene expression level was measured by RT-PCR. Number of mouse in each sample group=5. Statistical analysis within each groups was done by unpaired t-test, where **P<0.01 and*P<0.05

3.3.7. Selectivity of STR-KLGR modified YSK05-MEND to LSEC

This experiment was performed to evaluate selectivity of our developed carrier either to LSEC or hepatocyte. For this purpose we delivered Tie2 siRNA or FVII siRNA by either modified or unmodified YSK05-MEND to lower the gene expression of endothelial cell specific marker Tie2 gene or hepatocyte specific FVII factor respectively. The result shows that 0.5 mol% STR-KLGR modified YSK05-MEND successfully lowers Tie2 gene expression than FVII gene expression and the difference was statistically significant (fig. 3.6). We also compared the result with the knockdown efficiency of STR-R8

modified YSK05-MEND. It shows that STR-R8 modified YSK05-MEND caused lowering of gene expression of both the genes similarly.

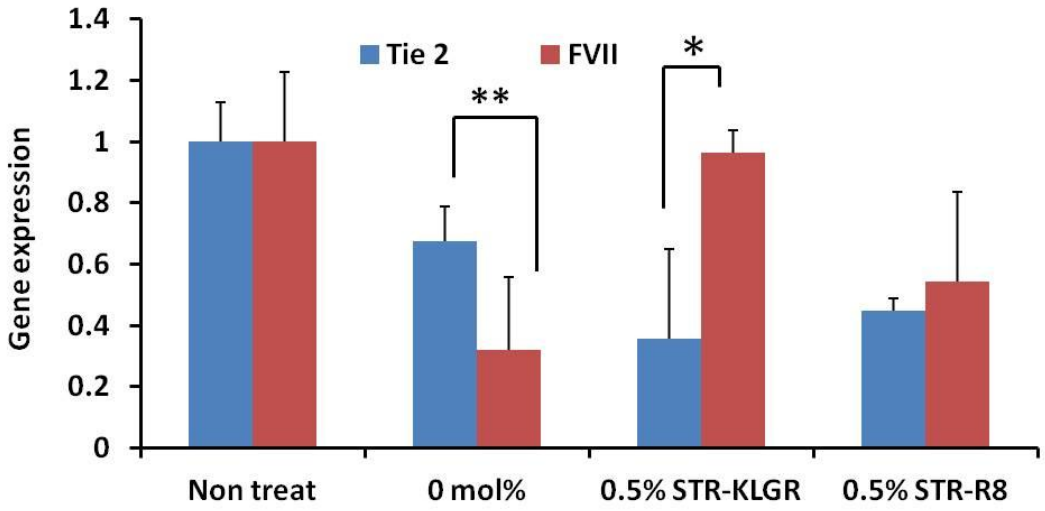

Figure 3.6: In vivo Tie2 and FVII gene expression by YSK05-MEND modified with 0.5 mol% of STR-KLGR or STR-R8 at the MEND surface. Male ICR mice were intravenously injected with YSK05-MEND modified with different mol% of STR-KLGR or STR-R8 encapsulating either Tie2 siRNA or FVII siRNA. After 24 hr of incubation liver samples were collected. After collecting mRNA from liver samples Tie2 or FVII gene expression level was measured by RT-PCR. Number of mouse in each sample group=4. Statistical analysis within each groups was done by unpaired t-test, where **P<0.01

3.3.8. Endosomal escape efficiency of STR-KLGR modified YSK05-MEND in LSEC

To evaluate the effect of different modification rate with STR-KLGR at YSK05-MEND on the intracellular trafficking efficiency, in vitro endosomal escape efficiency was measured by confocal microscopic image (fig. 3.9A-D). When we plotted the pixel count of 10 different cells in each group it was observed that the endosomal escape efficiency is maximum when the amount of ligand at the MEND surface is minimum (fig. 3.7E). It is seen that endosomal escape efficiency is highest at 0.5 mol% of modification with STR-KLGR at the nano carrier surface while at 1 mol% or 5 mol% modification with STR-KLGR decreases the endosomal escape efficiency of cy3 labeled Tie2 siRNA and the difference was statistically significant (fig. 3.7E).

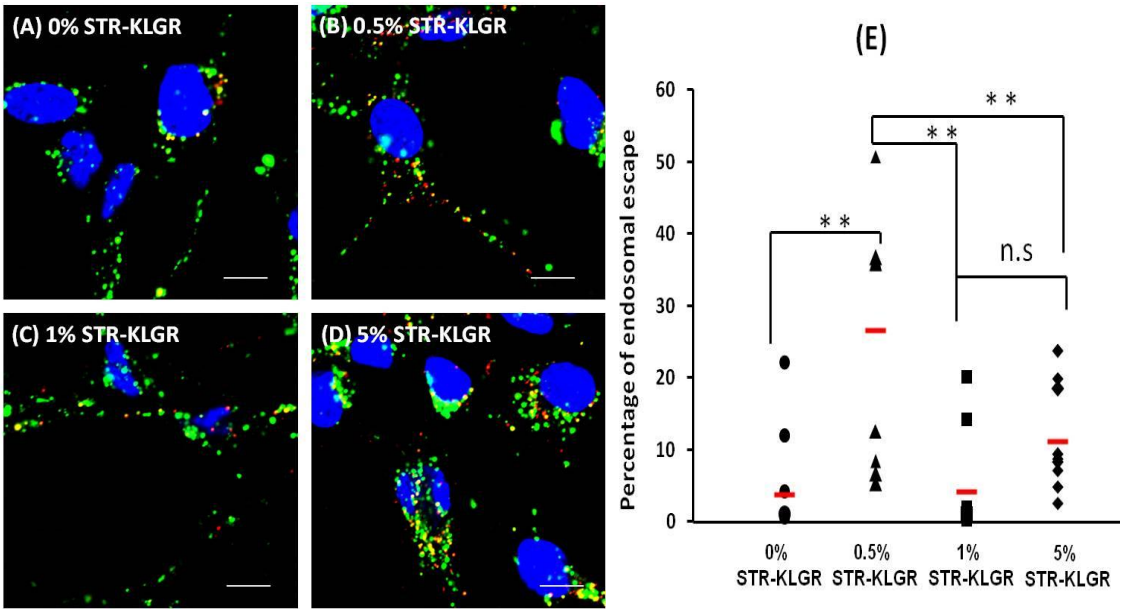

Figure 3.7: Endosomal escape efficiency of YSK05-MEND modified with (A) 0 mol%, (B) 0.5 mol%, (C) 1 mol% and (D) 5 mol%. MEND encapsulating cy3-labeled Tie 2 siRNA were transfected into LSECs. The endosomes/lysosomes (green) were stained with Lysotracker green to differentiate between siRNA in endosomes/lysosomes (yellow) and the cytosol (red). The fraction of siRNA in endosomes and the cytosol was quantified based on the pixel area of clusters in each region of interest, as described in section 4.2.11. (E) Quantitative comparison of endosome escape efficiency between each group where endosome escape efficiency in 10 individual cells was plotted. Red bars represent the average values. Statistical differences between groups were performed by ANOVA followed by SNK test where *p<0.01

3.3.9. Uptake mechanism study by confocal microscope

In vitro cellular uptake mechanism study was performed to find the intracellular fate of both modified and unmodified YSK05-MEND used for siRNA delivery in both LSEC and Hepa1-6 line. In this experiment different inhibitors were used to inhibit different uptake pathway. The inhibitors used here are given in table 4.2.

Table 3.2: List of inhibitors

Inhibitors	Used to inhibit
Amiloride	Macropinocytosis
Sucrose	Clathrin-mediated endocytosis
Filipin III	Caveolae-mediated endocytosis

It is reported that Amiloride inhibits macropinocytosis by inhibiting the Na+/H+ exchange required for macropinocytosis [91], a hypertonic sucrose solution inhibits clathrin-mediated endocytosis via dissociation of the clathrin lattice [92] and Filipin III inhibits caveolar uptake through cholesterol depletion [93]. A brief result of this experiment has been summarized in table 3.3.

It is shown from the fig. 3.8 that unmodified YSK05-MEND follows both macropinocytosis and clathrin-mediated endocytosis in LSEC (fig. 3.8.1) as well as in Hepa 1-6 cell line (fig. 3.8.2). When the YSK05-MEND is modified with 0.5 mol% of STR-KLGR then in LSEC it is following macropinocytosis or clathrin-mediated endocytosis in LSEC but in Hepa1-6 cell line it is following only clathrin-mediated endocytosis. The YSK05-MEND follows only clathrin-mediated endocytosis regardless of cell type when the surface of the MEND is modified with a higher density of ligand which is 5 mol%.

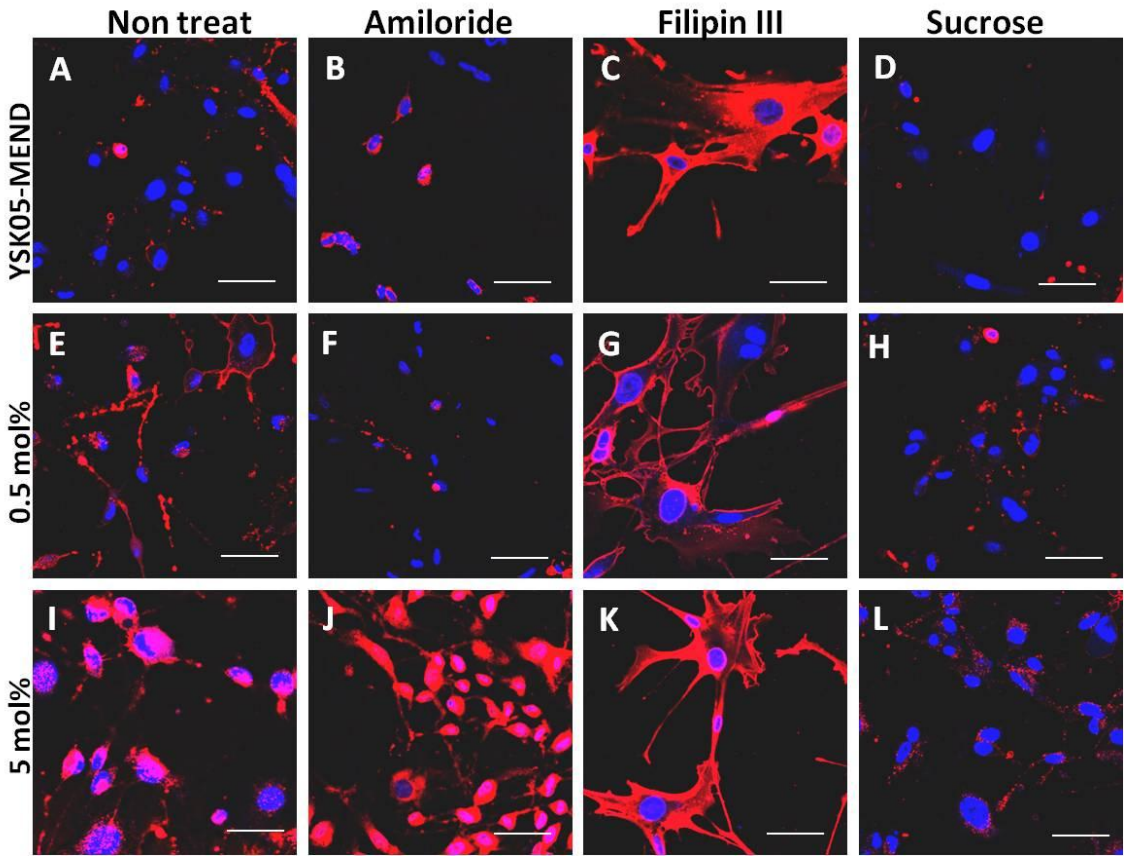

Figure 3.8.1: In vitro Uptake Mechanism of Rhodamin-DOPE labeled YSK05-MEND modified with (A-D) 0 mol%, (E-H) 0.5 mol%, and (I-L) 5 mol% in LSECs in presence or absence of three inhibitor amiloride, Filipin III and hypertonic Sucrose. Here red is for Rhodamin-DOPE labeled MEND and blue represents nucleus stained with Hoechst 33342.

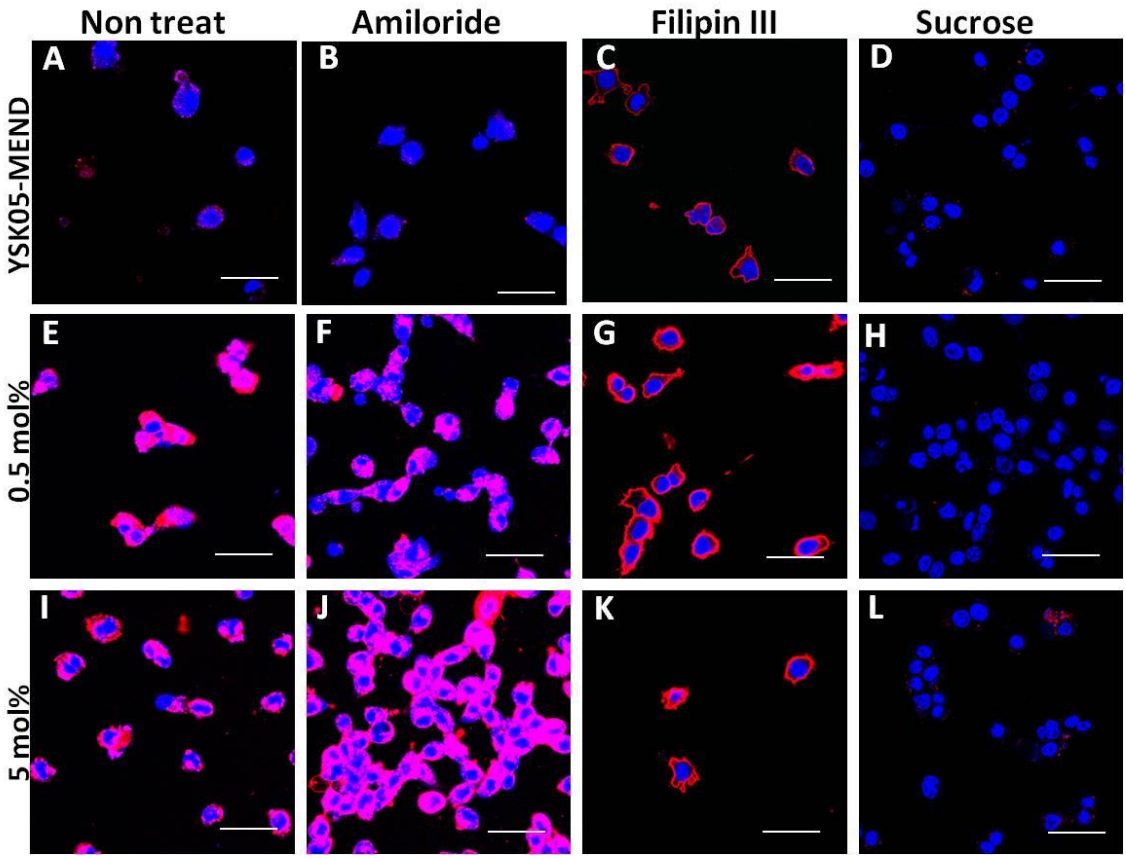

Figure 3.8.2: In vitro Uptake Mechanism of Rhodamin-DOPE labeled YSK05-MEND modified with (A-D) 0 mol%, (E-H) 0.5 mol%, and (I-L) 5 mol% in Hepa 1-6 cell line in presence or absence of three inhibitor amiloride, Filipin III and hypertonic Sucrose. Here red is for Rhodamin-DOPE labeled MEND and blue represents nucleus stained with Hoechst 33342.

Table 3.3: Summary result of uptake pathway

MEND	Uptake pathway	
	LSEC	Hepatocyte
Unmodified	1. Macropinocytosis 2. Clathrin mediated endocytosis	1. Macropinocytosis 2. Clathrin mediated endocytosis
0.5 mol% KLGR	1. Macropinocytosis 2. Clathrin mediated endocytosis	1. Clathrin mediated endocytosis
5 mol% KLGR	1. Clathrin mediated endocytosis	1. Clathrin mediated endocytosis

3.3.10. Selectivity of STR-KLGR to different types of endothelial cell

In this study the selectivity of 0.5 mol% STR-KLGR modified YSK05-MEND to endothelial cells in different tissues were measured. Here we find that 0.5 mol% STR-KLGR modified YSK05-MEND showed highest knockdown of Tie2 gene expression in endothelial cell in liver compared to lung or kidney and the difference was statistically significant (fig. 3.9).

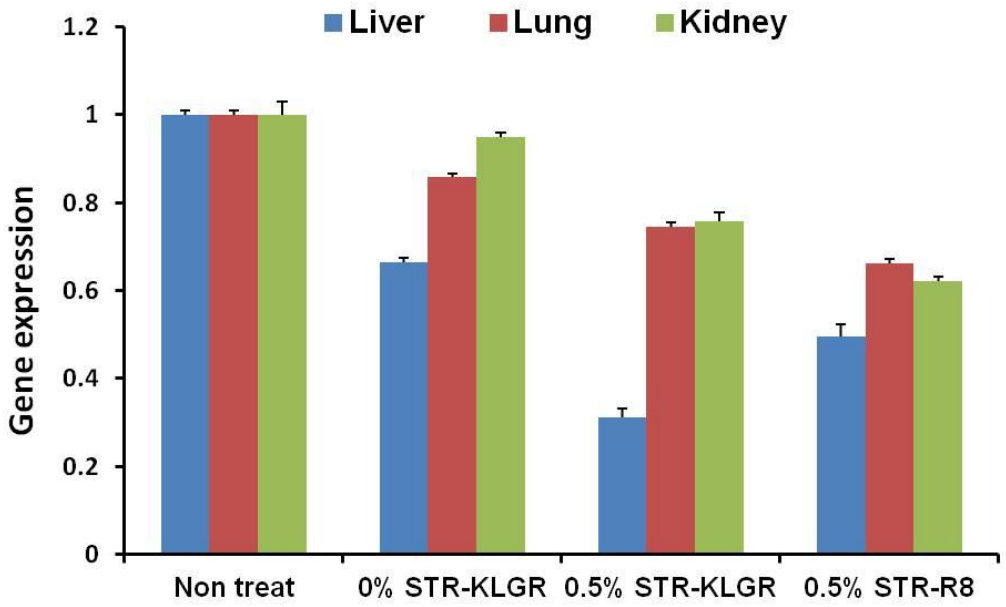

Figure 3.9: In vivo Tie2 gene expression by YSK05-MEND modified with 0. 5 mol% of STR-KLGR or STR-R8 into the endothelial cell of different tissues. Male ICR mice were intravenously injected with YSK05-MEND modified with 0.5 mol% of STR-KLGR or STR-R8 encapsulating Tie2 siRNA. After 24 hr of incubation liver, lung or kidney samples were collected. After collecting mRNA from the samples Tie2 gene expression level was measured by RT-PCR Number of mouse in each sample group=6.

3.3.11. Safety analysis of STR-KLGR modified YSK05-MEND

The safety analysis study was performed by measuring serum AST and ALT level after injecting 0.5 mol% STR-KLGR modified YSK05-MEND. The results shows that both unmodified and 0.5 mol% STR-KLGR modified YSK05-MEND did not show any significant difference in ALT and AST level compared to non treat group (fig. 3.10).

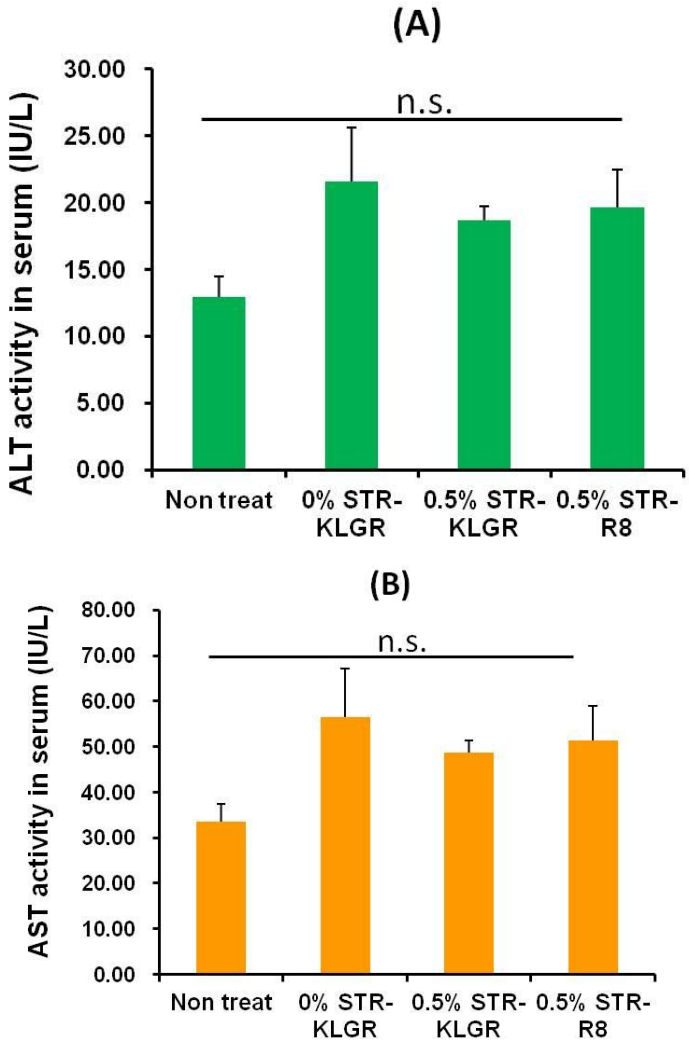

Figure 3.10: In vivo serum (A) AST or (B) ALT measurement after intravenous administration of YSK05-MEND modified with 0.5 mol% of STR-KLGR or STR-R8. Male ICR mice were intravenously injected with YSK05-MEND modified with 0.5 mol% of STR-KLGR or STR-R8 encapsulating Tie2 siRNA. After 24 hr of incubation blood samples were collected and serum AST and ALT level was measured. Statistical analysis Vs. non treat was done by ANOVA followed by Dunnett test, the differences were not significant.

3.4. Discussion

This study was aimed to develop a new LSEC targeted nanocarrier for siRNA delivery to LSEC which can successfully avoid lysosomal degradation and can achieve successful downregulation of an endothelial cell specific gene.

Though there are several approach for the gene delivery to liver a very few of them can be utilized to target LSEC. Moreover though some carrier can target LSEC specifically but ultimately fails to deliver gene to the cell cytosol [93].

In this experiment an attempt was made to prepare an LSEC selective nanocarrier for targeting LSEC. Here YSK05-MEND was used as a carrier for siRNA delivery. YSK05-MEND was previously reported from our lab. This MEND is made from a cationic lipid YSK05 which has fusogenic property. YSK05-MEND was reported to have a higher ability for endosomal escape than other MENDs containing conventional cationic lipids [93]. For modifying the surface of the MEND with an LSEC specific ligand we used KLGR peptide which has been reported in chapter 2. KLGR-PEG modified liposomal system showed high selectivity to LSEC. So at this study the surface of YSK05-MEND was modified with KLGR-PEG. But here PEG_{2000}-DSPE as a PEG linker. This type of PEG linker have some drawbacks in terms of endosomal escape efficiency. The major criteria for better endosomal escape efficiency is the fusion of the lipid bilayer of liposome or MEND with the endosomal lipid bilayer which will ultimately release the core material of the MEND into the cell cytosol (fig. 3.11A). But some PEG-linker inhibits the fusogenic property of the MEND. For successful fusion first the PEG should be shedded from the lipid bilayer of MEND. But in case of PEG2000-DSPE the double hydrocarbon chain of DSPE is attached to the lipid bilayer so tightly that it becomes impossible to shed the PEG (fig. 3.11B). And this phenomenon was previously termed as PEG-dilemma [95]. One previous report shows introduction of stearylated octaarginine (STR-R8) into the lipid envelope (R8-MEND) to enhance the cellular uptake of the MEND [96]. As an advance remedy of PEG dilemma we planned a parallel experiment with STR-KLGR modified YSK05-MEND.

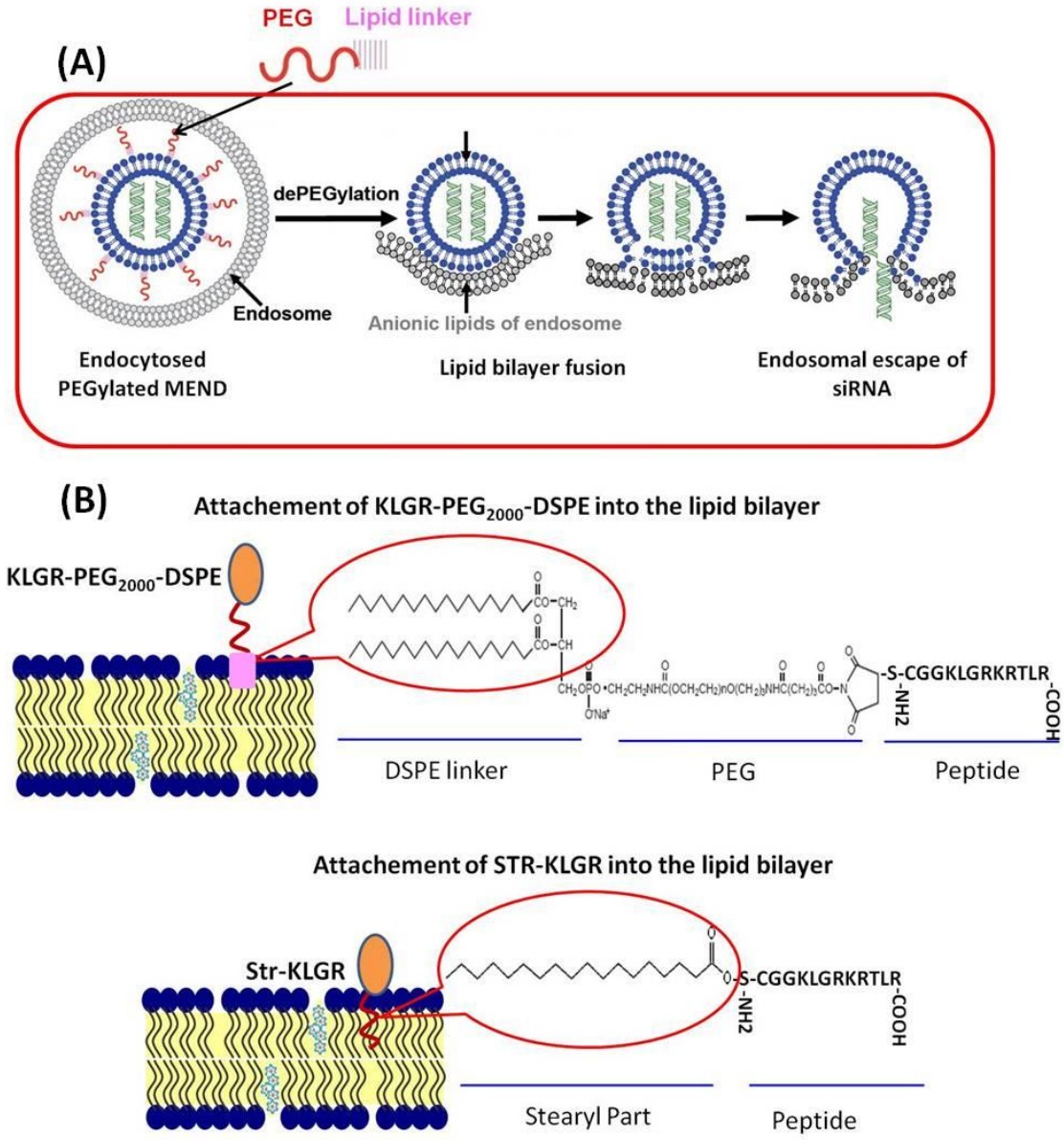

Figure 3.11: (A) Shematic representation of Endosomal escape. (B) Schematic representation of the attachment of KLGR-PEG and STR-KLGR at the surface of lipid bilayer of MEND

In vivo gene knockdown experiment shows that KLGR-PEG modified MEND could not achieve desired suppression of gene expression and we describe this as the effect of PEG-dilemma. But STR-KLGR modified MEND achieved 80% knockdown of Tie2 gene expression (fig. 3.2). It is notable that gene expression silencing activity increased with

the decrease in the amount of STR-KLGR at the surface of YSK05-MEND. To become sure about the uptake of the developed carrier we decided to do in vivo accumulation study by confocal microscope. In vivo confocal study shows that uptake of modified MEND increased with the increase in the amount of surface ligand (fig. 3.3). Here 0 mol% of STR-KLGR modified YSK05-MEND showed least accumulation through the blood vessel (fig. 3.3 A-B) where the 5mol% of STR-KLGR modified YSK05-MEND showed the most (fig. 3.3 G-H). Uptake study with flow cytometry also supported this data (fig. 3.4 A-B). Further gene silencing experiment with YSK05-MEND modified with lower amount of STR-KLGR such as 0.5 mol% or 0.1 mol% showed that 0.5 mol% STR-KLGR modified YSK05-MEND showed maximum knockdown efficiency (fig. 3.5). This data proves that for better siRNA delivery to LSEC the first criteria is to optimize the ligand amount for modification of carrier

For describing these reverse relationship with cellular uptake and gene silencing activity we took an effort to observe the endosomal escape efficiency of STR-KLGR modified YSK05-MEND. This experiment showed that YSK05-MEND modified with lower amount of STR-KLGR, i.e. 0.5 mol% can escape endosome more efficiently than 1 mol% or 5 mol% modification. This result can explain the reverse relationship with cellular uptake and gene silencing activity. As we see in the confocal image of endosomal escape efficiency experiment, for 5 mol% modification shows more merged signal of cy3 labeled siRNA with the acidic endosomal compartment in the cell cytosol than 0.5 mol% modification referring that there are more endosomal entrapment of 5 mol% STR-KLGR modified YSK05-MEND than other modification (fig. 3.7A-D). Graphical presentation of the pixel count of red and yellow area in the confocal microscopic image showed that there is highest endosomal escape for 0.5 mol% KLGR-PEG than 1 mol% or 5 mol% STR-KLGR modified YSK05-MEND (fig. 3.7E). This result can explain the reason behind low gene expression knock down at higher modification of ligand. Probably the low endosomal escape capacity of 5 mol% STR-KLGR modified YSK05-MEND reduces the ability of the MEND to release siRNA into the cell cytoplasm. So 0.5 mol% STR-KLGR- modified YSK05-MEND was able to achieve successful siRNA delivery to LSEC. This carrier also showed its selectivity to LSEC rather than hepatocyte as 0.5 mol% STR-KLGR- modified YSK05-MEND showed

better gene expression knockdown efficiency in LSEC rather than hepatocyte and the difference was statistically significant while 5 mol% STR-R8 modified YSK05-MEND showed similar gene expression knockdown efficiency in both LSEC and hepatocyte (fig. 3.6). Evaluation of uptake mechanism can reveal the reason of this selective siRNA delivery of 0.5 mol% STR-KLGR modified YSK05-MEND to LSEC.

In vivo cellular uptake mechanism shows that unmodified YSK05-MEND is internalized into the cell via macropinocytosis and clathrin-mediated endocytosis both in LSEC (fig. 3.8.1A-D) and Hepa1-6 cell line (fig. 3.8.2A-D). When the surface ligand density is low (0.5 mol %) then the carrier is internalized into LSEC by macropinocytosis and clathrin-mediated endocytosis (fig. 3.8.1E-H) but it follows clathrin-mediated endocytosis in Hepa1-6 (fig. 3.8.2E-H). But when the ligand density is higher it follows clathrin-mediated endocytosis (fig. 3.8.1I-L, 3.8.2I-L). As Clathrin-mediated endocytosis is susceptible to lysosomal degradation [97] (fig. 3.12 B) so YSK05-MEND containing high density of ligand at its surface fails to deliver siRNA regardless of cell type. At low density of ligand modified YSK05-MEND follows macropinocytosis in LSEC which is less susceptible to lysosomal degradation [98] (fig. 3.12 A) but in hepatocyte it is taken up via clathrin-mediated endocytosis. May be this is the possible cause of successful knockdown of gene expression in LSEC than hepatocyte (fig. 3.6) by 0.5 mol% of STR-KLGR modified YSK05-MEND. While unmodified YSK05-MEND follows macropinocytosis in both type of cell. So they did not show specificity to any of the cells (fig. 3.6). Above all, 0.5 mol % STR-KLGR modified YSK05-MEND successfully target LSEC and can deliver siRNA to the cell cytosol avoiding lysosomal degradation and showed acceptable knockdown efficiency of an endothelial cell specific gene. This system also showed its safety comparable to non treated mice (fig. 3.10A-B). Considering all these data it was assumed that the developed STR-KLGR modified YSK05-MEND can become an effective tool for gene therapy targeting LSEC.

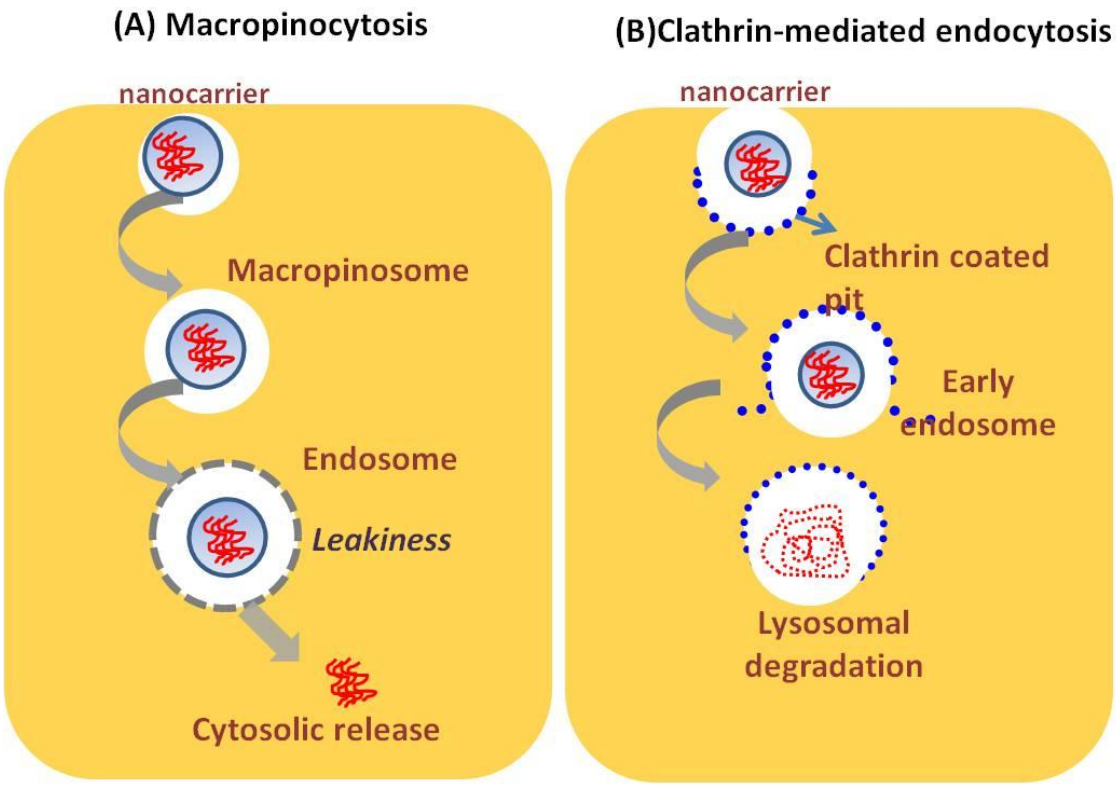

Figure 3.12: Graphical representation of (A) Macropinocytosis and (B)Clathrin-mediated endocytosis

3.5.Conclusion

For developing a successful targeted gene carrier for LSEC for siRNA therapy three basic parameter should be considered and they are ligand densiy at the nanocarrier surface, endosomal escape efficiency and the uptake mechanism of the carrier into the targeted cell. Considering these three points STR-KLGR modified YSK05-MEND successfully met all the three points which make us to believe that this delivery system can be studied further to suppress disease related gene into the LSECs.

Summary of the study

Liver sinusoidal endothelial cells (LSECs) are the distinctive cells residing in the sinusoid of liver. They separate hepatocytes from blood circulation. LSECs are very different from other cell types in having fenestration. They separate an array of physiological and also foreign molecules and colloidal substances from blood circulation. Besides physiological function they also play role in many pathophysiological condition, such as, hepatitis, fibrosis, cirrhosis, alcoholic liver diseases etc. By secreting different inflammatoty molecules they induce inflammation which ultimately causes cell death. In this study my aim was to develop an LSEC targeting nanocarrier which will specifically target LSEC and deliver its cargo to the cell cytosol.

For the designing of an LSEC targeting nanocarrier first I designed a ligand specific for LSEC. For this, we designed the ligand from ApoB-100 sequence (3359-3367) of LDL molecule which is actually responsible for binding of LDL molecule with LDL receptor. As LDL molecules are taken up by LSECs so I designed one peptide ligand from this sequence and named as RLTR. Another peptide ligand was designed from the reverse sequence of RLTR and was named as KLGR peptide. Peptide was conjugated with maleimide-PEG_{2000}-DSPE to synthesize RLTR-PEG_{2000}-DSPE or KLGR-PEG_{2000}-DSPE. RLTR-PEG modified EPC/Cholesterol liposome (RLTR-PEG-LP) was taken up by both primary mouse LSEC and Hepa1-6 (mouse epithelial hepatoma cell). In vivo confocal microscopy image shows that liposomes were only accumulated through the blood vessels but not in the hepatocyte. Both in vivo and in vitro inhibiton study showed that both the RLTR and KLGR modified PEG-LP were accumulated through blood vessels and their uptake was inhibited by unlabeled RLTR or KLGR modified PEG-LP. However, the cationic LPs did not affect its uptake both in vivo and in vitro. The possible reason may be, only the cationic charge of the peptide modified PEG-LP is not responsible for accumulation but also sequence of the peptide is playing the key role to target LSEC. Biodistribution study shows superiority of KLGR peptide over RLTR. So we selected KLGR peptide for the next study of development of a specific nanocarrier for gene delivery to LSEC.

For the siRNA delivery study to LSEC I took an attempt to deliver Tie2 siRNA to LSEC to lower the expression of Tie2 gene (a specific gene to all type of endothelial cell). For delivering siRNA we modified previously reported fusogenic YSK05-MEND from our lab with stearylated-KLGR (STR-KLGR). Here we replaced KLGR-PEG as it showed almost no decrease in gene expression due to the effect of peg-dilemma. STR-KLGR modified YSK05-MEND showed decrease in the Tie2 gene expression and the decrease was most when the ligand density was low at the MEND surface. 0.5 mol% of STR-KLGR at MEND surface showed better knock down effect than other higher modification like 1 mol% or 5 mol% though both in vitro and in vivo experiment showed that the uptake of YS05-MEND increases into LSEC with the increase of the mol% of STR-KLGR at the MEND surface. This was due to the lower endosomal escape efficiency of MEND containing high density of ligand at their surface. Endosomal escape efficiency study shows that only 0.5 mol% STR-KLGR modified YSK05-MEND could successfully escape from the endosome. Uptake mechanism study explains this fact as the MEND modified with low density of ligand at their surface follows macropinocytosis can deliver the siRNA successfully into the cell cytosol whereas MEND modified with high density of ligand follows clathrin-mediated endocytosis which is susceptible for lysosomal degradation. Thus the 5mol% STR-KLGR modified could not show acceptable knock down in gene expression but 0.5 mol% STR-KLGR showed significant knock down of Tie2 gene expression. The developed nanocarrier also showed its safety comparable to non treat. Therefore, the newly developed 0.5 mol% STR-KLGR modified YSK05-MEND can become a useful tool for delivering siRRNA to LSECs.

References

1. Handbook of Medical physiology, 11th edition, by-Guyton and Hall, chapter 70, page: 859-864

2. Wisse E, Geerts A , Cell biology of liver endothelial and Kupffer cells. , Smedsrød B, De Bleser PJ, Braet F, Lovisetti P, Vanderkerken K, Gut 1994; 35:1509-151

3. Kjetil Elvevold, Bard Smedsrød, and Inigo Martinez, The liver sinusoidal endothelial cell: a cell type of controversial and confusing identity, Am J Physiol Gastrointest Liver Physiol 2008; 294: G391–G400,

4. G. Ramadori, F. Moriconi, I. Malik, J.Dudas, Physiology and pathophysiololgy of liver inflammation, damage and repair, Journal of physiology and pharmacology, 2008; 59:107-117

5. Patric B, Geoffray WM and David GB, Role of primary intrahepatic T-cell activation in the 'liver tolerance effect', Immunology and Cell Biology 2002; 80: 84-92

6. Kmiec, Z. Cooperation of liver cells in health and disease, Adv Anat Embryol Cell Biol 2001; 161(III-XIII): 1-151.

7. Wisse E. An electron microscopic study of the fenestrated endothelial lining of rat liver sinusoids. J Ultrastruct Res. 1970; 31: 125–50.

8. Wisse E. An ultrastructural characterization of the endothelial cell in the rat liver sinusoid under normal and various experimental conditions, as a contribution to the distinction between endothelial and Kupffer cells. J Ultrastruct Res. 1972; 38: 528–62.

9. DeLeve LD, Vascular Liver Disease: Mechanisms and Management, 2011, 25-40

10. March S, Hui EE, Underhill GH, Khetani S, Bhatia SN, Microenvironmental Regulation of the Sinusoidal Endothelial Cell Phenotype In Vitro, Hepatology. 2009; 50(3): 920-8

11. PF Lalor, WK Lai, SM Curbishley, S Shetty, DH Adams, Human hepatic sinusoidal endothelial cells can be distinguished by expression of phenotypic markers related to their specialised functions in vivo, World J Gastroenterol 2006 12(34): 5429-5439

12. Vaporciyan AA, DeLisser HM, Yan HC, Mendiguren II, Thorn SR, Jones ML, et al. Involvement of platelet- endothelial cell adhesion molecule-1 in neutrophil recruitment in vivo. Science. 1993; 262:1580-2.

13. DeLeve LD, Wang X, Hu L, McCuskey MK, McCuskey RS. Rat liver sinusoidal endothelial cell phenotype is under paracrine and autocrine control. Am J Physiol Gastrointest Liver Physiol. 2004; 287: G757–63.

14. Harb R, Xie G, Lutzko C, Guo Y, Wang X, Hill C, et al. Bone marrow progenitor cells repair rat hepatic sinusoidal endothelial cells after liver injury. Gastroenterology. 2009;137:704–12

15. Scoazec JY, Feldmann G. In situ immunophenotyping study of endothelial cells of the human hepatic sinusoid: results and functional implications. Hepatology. 1991; 14:789–97.

16. Filip B and Wisse E, Structural and functional aspects of liver sinusoidal endothelial cell fenestrae: a review, Comparative Hepatology 2002, 1: 1-17

17. Oda M, Tsukada N, Watanabe N, Komatso H, Yonei Y, Tsuchiya M, Functional implications of the sinusoidal endothelial fenestrae in the regulation of the hepatic microcirculation. Hepatology 1984; 4:754

18. Oda M, Tsukada N, Komatsu H, Yonei Y, Honda K, Tsuchiya M: Mechanism of contraction and dilatation of sinusoidal endothelial fenestrae in the liver. Hepatology 1986; 6:771

19. Arias IM: The biology of hepatic endothelial cell fenestrae. In: Progress in Liver Diseases IX (Edited by: Schaffer F, Popper H) Philadelphia, WB Saunders 1990; 11-26

20. Schaffner F, Popper H. Capillarization of hepatic sinusoids in man. Gastroenterology 1963; 44:239-42.

21. Dubuisson L, Boussarie L, Bedin C-A, Balabud C, Bioulac-Sage P. Transformation of sinusoids into capillaries in a rat model of selenium-induced nodular regenerative hyperplasia: an immunolight and immunoelectron microscopic study. Hepatology1995; 21: 805–14.

22. Arias IM: The biology of hepatic endothelial cell fenestrae. In: Progress in Liver Diseases IX (Edited by: Schaffer F, Popper H) Philadelphia, WB Saunders 1990, 11-26

23. Breiner KM, Schaller H, Knolle PA, Endothelial cell-mediated uptake of a hepatitis B virus: a new concept of liver targeting of hepatotropic microorganisms. Hepatology. 2001; 34(4 Pt 1):803-8.

24. Kruse N, Neumann K, Schrage A, Priming of CD4_ T Cells by Liver Sinusoidal Endothelial Cells Induces CD25^{low} Forkhead Box Protein 3–Regulatory T Cells Suppressing Autoimmune Hepatitis, Hepatology. 2009; 50(6):1904-13

25. I Rowe, P Lalor, D Adams, P Balfe, J McKeating, OP23 Vascular endothelial growth factor activation of liver sinusoidal endothelial cells via vascular endothelial growth factor receptor-2 regulates hepatocellular hepatitis C virus replication, Gut 2010; 59:A10

26. Anchony PP, Ishak KG, Nayak NC, Poulsen HE, Scheuer PJ, Sobin LH: The morphology of cirrhosis. J Clin Pathol 1978, 31:395-414

27. Hao Xu, Bao-Min Shi, and Jian Xu, Vascular endothelial growth factor attenuates hepatic sinusoidal capillarization in thioacetamide-induced cirrhotic rats, world J Gastroenterol, 2008, 14(15): 2349-2357

28. Cogger VC, Warren A, Fraser R, Ngu M, McLean AJ, Le Couteur DG. Hepatic sinusoidal pseudocapillarization with aging in the non-human primate. Exp Gerontol. 2003; 38:1101-7.

29. Martens JH, Kzhyshkowska J, Falkowski-Hansen M, Schledzewski K, Gratchev A, Mansmann U, et al. Differential expression of a gene signature for scavenger/ lectin receptors by endothelial cells and macrophages in human lymph node sinuses, the primary sites of regional metastasis. J Pathol. 2006; 208:574-89

30. Horn T, Christoffersen P, Henriksen JH, Alcoholic liver injury: defenestration in noncirrhotic livers--a scanning electron microscopic study. Hepatology. 1987; 7(1):77-82.

31. Kanaoka H, Okanoue T, Ohta M, Kachi K, Sawa Y, Ou O, Kagawa K, Yuki T, Okuno T, Takino T: Scanning electron microscopy of endothelial fenestration in liver sinusoids of rats fed ethanol. Electron Microscopy 1986; 2919-1920

32. Fraser R, Bowler LM, Wisse E: Agents related to fibrosis, such as alcohol and carbon tetrachloride, acutely effect endothelial fenestrae which cause fatty liver. Connective Tissue of the Normal and Fibrotic Human Liver (Edited by: Gerlach V, Pott J, Rauterberg J, Vob B) Stuttgart, Thierne G verlag 1982, 159-160

33. Ramadori, G., Moriconi, F., Malik, I., Dudas, J., Physiology and pathophysiology of liver inflammation, damage and repair. J Physiol Pharmacol 2008;. 59, 107-117

34. Leonardo G, Mangia A, Hui J,Relationship Between Steatosis et al, Inflammation, and Fibrosis in Chronic Hepatitis C: A Meta-Analysis of Individual Patient Data. Gastroenterology 2006;130:1636–1642

35. Robinson WS. Hepatitis B viruses. General Features (human). In: Webster RG and Granoff A, eds. Encyclopedia of Virology, London, Academic Press Ltd, 1994: 554-569.

36. Autschbach F, Meuer SC, Moebius U, Manns M, Hess G, Meyer zum Buschenfelde KH, et al. Hepatocellular expression of lymphocyte function-associated antigen 3 in chronic hepatitis. Hepatology 1991; 14:223–230.

37. Crawford JM, Histologic findings in alcoholic liver disease. Clin Liver Dis. 2012; 16(4):699-716.

38. Ren X, Kennedy A, Colletti LM. CXC chemokine expression after stimulation with interferon-gamma in primary rat hepatocytes in culture. Shock 2002; 17: 513-520.

39. Li X, Klintman D, Liu Q, Sato T, Jeppsson B, Thorlacius H. Critical role of CXC chemokines in endotoxemic liver injury in mice. J Leukoc Biol 2004; 75: 443-452.

40. Hermann EW, Frank L, Mirko MZ, Ralf W et al., Antifibrotic Effects of CXCL9 and Its Receptor CXCR3 in Livers of Mice and Humans, Gastroenterology 2009;137(1): 309–319

41. Grisham JW, Nopanitaya W, Compagno J, Nagel AE. Scanning electron microscopy of normal rat liver: the surface structure of its cells and tissue components. Am J Anat 1975; 144: 295-321.

42. Sheikh N, Tron K, Dudas J, Ramadori G. Cytokine-induced neutrophil chemoattractant-1 is released by the non-injured liver in a rat acute-phase model. Lab Invest 2006; 86: 800-814.

43. Koj A. Cytokines regulating acute inflammation and synthesis of acute-phase proteins. Blut 1985; 51:267–274.

44. Ramadori G, Christ B. Cytokines and the hepatic acute-phase response. Semin Liver Dis 1999; 19:141–155.

45. Neumann K, Kruse N, Wechsung K et al., Chemokine presentation by liver sinusoidal endothelial cells as therapeutic target in murine T cell-mediated hepatitis, Z Gastroenterol 2011; 49 - V04

46. Samantha Y, Hidekazu T, and Vijay K. K. Ethanol-Induced Expression of ET-1 and ET-BR in Liver Sinusoidal Endothelial Cells and Human Endothelial Cells Involves Hypoxia-Inducible Factor-1α and MicroRNA-199, J Immunol 2009; 5232-5243

47. K Neubauer, T Wilfling, A Ritzel, G Ramadori, Platelet-endothelial cell adhesion molecule-1 gene expression in liver sinusoidal endothelial cells during liver injury and repair. J Hepatol. 2000; 32(6):921-32.

48. Knittel T, Dinter C, Kobold D et al. Expression and regulation of cell adhesion

molecules by hepatic stellate cells (HSC) of rat liver: involvement of HSC in recruitment of inflammatory cells during hepatic tissue repair. Am J Pathol 1999; 154: 153-167

49. Kolios G, Valatas V, Kouroumalis E, Role of Kupffer cells in the pathogenesis of liver disease, World J Gastroenterol 2006; 12 (46): 7413-7420

50. Akhtar S, Benter IF.Nonviral delivery of synthetic siRNAs in vivo. J Clin Invest. 2007; 117(12):3623-32.

51. Leng Q, Woodle MC, Lu PY, Mixson AJ. Advances in Systemic siRNA Delivery. Drugs Future. 2009; 34(9):721.

52. A Akinc, R. Langer, Measuring the pH environment of DNA delivered using nonviral vectors: implications for lysosomal trafficking, Biotechnol. Bioeng. 2002; 78 (5): 503-508.

53. T. Kakudo, S. Chaki, S. Futaki, I. Nakase, K. Akaji, T. Kawakami, K. Maruyama, H. Kamiya, H. Harashima, Transferrin-modified liposomes equipped with a pHsensitive fusogenic peptide: an artificial viral-like delivery system, Biochemistry 2004; 43 (19):5618-5628.

54. Bumcrot D, Manoharan M, Koteliansky V, Sah DW. RNAi therapeutics: a potential new class of pharmaceutical drugs. Nat Chem Biol 2006; 2: 711-9

55. Zender L, Kubicka S. Suppression of apoptosis in the liver by systemic and local delivery of smallinterfering RNAs. Methods Mol Biol 2007; 361:217-226.

56. Song E, Lee SK, Wang J, Ince N, Ouyang N, Min J, et al. RNA interference targeting Fas protects mice from fulminant hepatitis. Nat Med 2003;9(3):347-351.

57. Soriano P, Dijkstra J, Legrand A, Spanjer H, Londos-Gagliardi D, Roerdink F, et al. Targeted and nontargeted liposomes for in vivo transfer to rat liver cells of a

plasmid containing the preproinsulin I gene. Proc Natl Acad Sci USA 1983; 80(23):7128-7131.

58. Leng Q, Woodle MC, Lu PY, Mixson AJ., Advances in Systemic siRNA Delivery. Drugs Future. 2009; 34(9):721.

59. Kim SI, Shin D, Choi TH, Lee JC, Cheon GJ, Kim KY, et al. Systemic and specific delivery of small interfering RNAs to the liver mediated by apolipoprotein A-I. Mol Ther 2007; 15(6):1145-1152.

60. Watanabe T, Umehara T, Yasui F, Nakagawa S, Yano J, Ohgi T, et al. Liver target delivery of small interfering RNA to the HCV gene by lactosylated cationic liposome. J Hepatol 2007; 47(6):744- 750.

61. Morrissey, D.V., Lockridge, J.A., Shaw, L., Blanchard, K., Jensen, K., Breen, W., et al. Potent and persistent in vivo anti-HBV activity of chemically modified siRNAs. Nat. Biotechnol. 2005; 23, 1002-1007

62. K. Kogre, H. Akita, H. Harashima, Multifunctional envelope-type nano device for non-viral gene delivery: concept and application of programmed packaging, J. Control. Release 2007; 122 (3):46-251.

63. K. Kogre, H. Akita, Y. Yamada, H. Harashima, Multifunctional envelope-type nano device (MEND) as a non-viral gene delivery system, Adv. Drug Deliv. Rev. 2008; 60 (4–5): 559-571.

64. Khalil, K. Kogure, S. Futaki, H. Harashima, High density of octaarginine stimulates macropinocytosis leading to efficient intracellular trafficking for gene expression, J. Biol. Chem. 2006; 281(6):3544-3551.

65. Khalil IA, Hayashi Y, Mizuno R, Harashima H. Octaarginine- and pH sensitive fusogenic peptide-modified nanoparticles for liver gene delivery. J Control Release.

2011; 56(3):374-80.

66. Targeted gene delivery to sinusoidal endothelial cells: DNA nanoassociate bearing hyaluronan-glycocalyx, Takei Y, Maruyama A, Ferdous A, Nishimura Y, et al., FASEB J. 2004;18(6):699-701.

67. Dominique, T., Vijay, S., Intrahepatic angiogenesis and sinusoidal remodeling in chronic liver disease: New targets for the treatment of portal hypertension? J Hepatol. 2010; 6-980.

68. Rajkumar, C., Gerene, MD., Gee, W., L., Michael, C., G., Sarah, N., H., David, G., Le, C., athogenesis of the hyperlipidemia of Gram-negative bacterial sepsis may involve athomorphological changes in liver sinusoidal endothelial cells. Int. J. Infect. Dis. 2010; 857-867

69. Brown, M., S., Deuel, T., F., Basu, S., K., Goldstein, J., L., Inhibition of binding of low density lipoprotein to its cell surface receptors in human fibroblasts by positively charged proteins. J Supramol Struct. 1978; 3-234

70. Urban, O., German, C., Eva, H., C., Karin, E., Goran, B., Possible Functional Interactions of Apolipoprotein B-100 Segments That Associate With Cell Proteoglycans and the ApoB/E Receptor. Arterioscler Thromb Vasc Biol. 2010; 17, 149-152

71. Urban, O., German, C., Goran, B. Binding of a synthetic Apolipoprotein B-100 peptide and peptide Analogues to Chondroitin 6-Sulfate: Effects of the Lipid Environment. Biochemistry 1993; 32, 1858-1865

72. Oie, C., I., Appa, R., S., Hilden, I., Petersen, H., H., Gruhler, A., Smedsrød, B., Rat liver sinusoidal endothelial cells (LSECs) express functional low density lipoprotein receptor related protein-1 (LRP-1). J Hepatol. 2011; 55, 1346–1352

73. Thomas, E., W., Anders, N., Joachim H. Lipoprotein receptors: new roles for ancient proteins. Nat Cell Biol. 1999; 1, 157-162

74. Marit, S., N., Rune, B., Christian, A., D., Grete, M., K., Kaare R., N., Trond B., 1998. Uptake of LDL in parenchymal and non-parenchymal rabbit livercells in vivo. Biochem. J. 1998; 254, 443-448

75. Puri, A., Loomis, K., Smith, B., Lee, J.,H., Yavlovich, A., Heldman, E. Lipid-Based Nanoparticles as Pharmaceutical Drug Carriers: From Concepts to Clinic. Crit Rev Ther Drug Carrier Syst 2009; 26, 523-580

76. Du, S.,L., Pan, H., Lu, W.,Y., Wang, J, W., J., Wang, J., Y. Cyclic Arg-Gly-Asp peptide labeled liposomes for targeting drug therapy of hepatic fibrosis in rats. J Pharmacol Exp Ther. 2007; 322 : 560-568

77. Ishiwata H, Suzuki N, Ando S, Kikuchia H, Kitagawa T, Characteristics and biodistribution of cationic liposomes and their DNA complexes. Journal of Controlled Release 2000; 69: 139-148

78. Hida, K., Hida, Y., Amin D.N., Flint, A.F., Panigrahy, D., Mortonet, C.C. Tumor-associated endothelial cells with cytogenetic abnormalities. Cancer Res. 2004; **64**,8249–8255

79. Akino, T., Hida, K., Hida, Y., Tsuchiya, K., Freedman, D., Muraki, C. Cytogenetic abnormalities of tumor-associated endothelial cells in human malignant tumors. Am J Pathol. 2009; 75, 2657-2667

80. Ohga, N., Hida, K., Hida, Y., Muraki, C., Tsuchiya, K., Matsuda, K. Inhibitory effects of epigallocatechin-3 gallate, a polyphenol in green tea, on tumor-associated endothelial cells and endothelial progenitor cells, Cancer Sci. 2009; 100, 1963-1970

81. Hatakeyama, H., Akita, H., Maruyama, K., Suhara, T., Harashima, H. Factors governing the in vivo tissue uptake of transferring-coupled polyethylene glycol liposomes in vivo. Int J Pharm. 2004; 281, 25-33

82. Kibria, G., Hatakeyama, H., Harashima, H. A new peptide motif present in the protective antigen of anthrax toxin exerts its efficiency on the cellular uptake of liposomes and applications for a dual-ligand system. Int J Pharm. 2011;

412:106-114

83. Kmieć, Z. Cooperation of liver cells in health and disease, Adv Anat Embryol Cell Biol. 2001; 161:1-151

84. Bartsch, M., Weeke-Klimp, A.,H., Hoenselaar, E.,P., Stuart, M.,C., Meijer, D.,K., Scherphof, G.,L., Kamps, J.,A. Stabilized Lipid Coated Lipoplexes for the Delivery of Antisense Oligonucleotides to Liver Endothelial Cells In Vitro and In Vivo, J Drug Target. 2004; 12:613–621

85. Toriyabe, N., Hayashi, Y., Hyodo, M., Harashima, H., 2011. Synthesis and evaluation of stearylated hyaluronic acid for the active delivery of liposomes to liver endothelial cells. Biol Pharm Bull. 2011; 34:1084-1089

86. Lehto, T., Abes, R., Oskolkov, N., Suhorutšenko, J., Copolovici, D. M. Delivery of nucleic acids with a stearylated (RxR)4 peptide using a non-covalent co-incubation strategy. J Control Release. 2010;141:42–51

87. Eva HC, Olsson, O., Olov, W., Coran, B., German, C. Cellular consequences of the association of Apo B Lipoproteins with Proteoglycans, Potential contribution to Atherogenesis. Arterioscler Thromb Vasc Biol. 1997; 17:1011-1017

88. Oshita, M., Sato, N., Yoshihara, H., Takei, Y., Hijioka, T., Fukui, H., Goto, M., Matsunaga, T., Kawano, S., Fusamoto, H., et al., Ethanol-induced vasoconstriction causes focal hepatocellular injury in the isolated perfused rat liver. Hepatology 1992; 16:1007.1013

89. Sato Y, Hatakeyama H, Sakurai Y, Hyodo M, Akita H, Harashima H., A pH-sensitive cationic lipid facilitates the delivery of liposomal siRNA and gene silencing activity in vitro and in vivo. J Control Release. 2012; 163(3):267-76.

90. Toriyabe N, Hayashi Y, Harashima H., The transfection activity of R8-modified nanoparticles and siRNA condensation using pH sensitive stearylated-octahistidine. Biomaterials 2013; 34(4):1337-43.

91. L.J. Hewlett, A.R. Prescott, C. Watts, The coated pit and macropinocytic pathways serve distinct endosome populations, J. Cell Biol. 1994; 124: 689–703.

92. J.E. Heuser, R.G. Anderson, Hypertonic media inhibit receptor-mediated endocytosis by blocking clathrin-coated pit formation, J. Cell Biol. 1989; 108: 389–400.

93. Lamaze, S.L. Schmid, The emergence of clathrin-independent pinocytic pathways, Curr. Opin. Cell Biol. 1995; 7:573–580.

94. Bartsch M, Weeke-Klimp AH, Hoenselaar EP, Stuart MC, Meijer DK, Scherphof GL, Kamps JA. Stabilized lipid coated lipoplexes for the delivery of antisense oligonucleotides to liver endothelial cells in vitro and in vivo. J Drug Target. 2004; 12(9-10):613-21.

95. Hatakeyama H, Akita H, Harashima H. A multifunctional envelope type nano device (MEND) for gene delivery to tumours based on the EPR effect: a strategy for overcoming the PEG dilemma. Adv Drug Deliv Rev. 2011; 63(3):152-60.

96. K. Kogure, H. Akita, H. Harashima. Multifunctional envelope-type nano device for non-viral gene delivery: concept and application of Programmed Packaging, J. Control. Release 2007; 122, pp. 246–251

97. McMahon HT, Boucrot E. Molecular mechanism and physiological functions of clathrin-mediated endocytosis. Nat Rev Mol Cell Biol. 2011; 12(8):517-33

98. Yu B, Hsu SH, Zhou C, Wang X, Terp MC, Wu Y, Teng L, Mao Y, Wang F, Xue W, Jacob ST, Ghoshal K, Lee RJ, Lee LJ. Lipid nanoparticles for hepatic delivery of small interfering RNA. Biomaterials. 2012; 33(25):5924-34.

List of Figures

Chapter 1

Chapter 2

Chapter 3

List of Tables

Chapter 1

Chapter 2

Chapter 3

APPENDIX

Chemical Structure of lipids used in this study

Egg phosphatidylcholine (EPC)

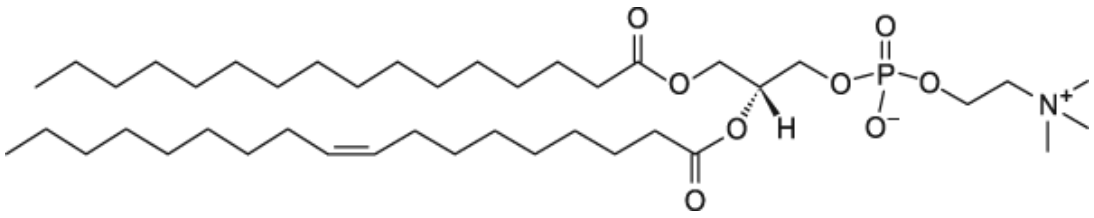

Cholesterol

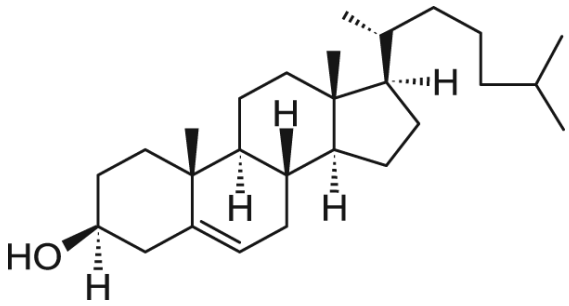

DSPE-PEG2000

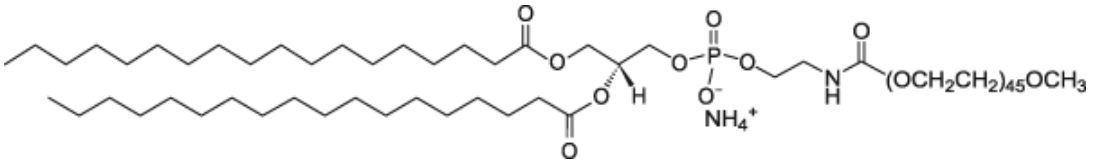

YSK05 lipid

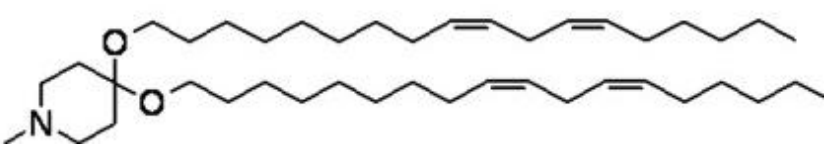

Rhodamine-DOPE

(1,2-dioleoyl-*sn*-glycero-3-phosphoethanolamine-N-(lissamine rhodamine B sulfonyl) (ammonium salt))

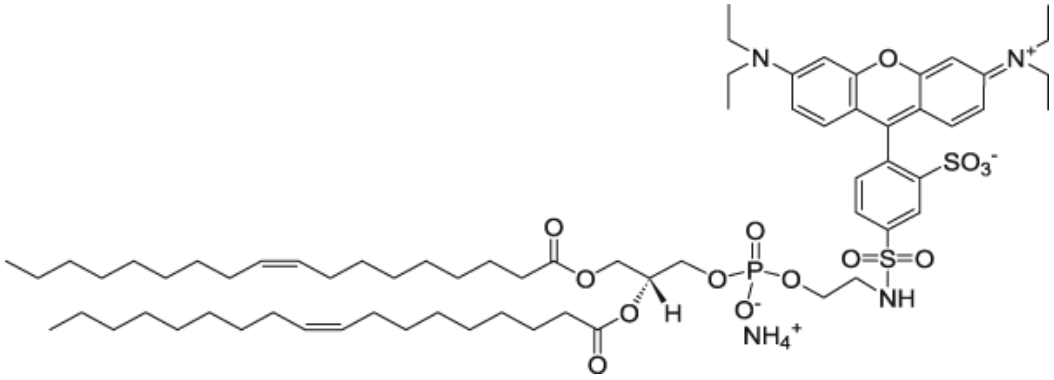

Maleimide-PEG-DSPE

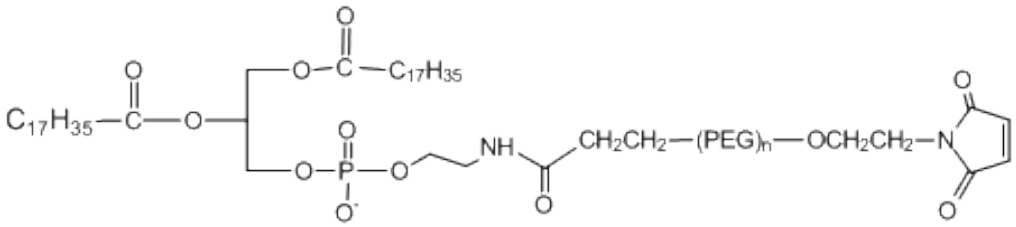

Abbreviations

A

ALD: Alcoholic Liver Disease

ALT: Alanine aminotransferase

Apo B: Apolipoprotein B

AST: Aspartate aminotransferase

C

CLSM: Confocal Laser Scanning Microscopy

CSPG: Chondroitin sulphate rich proteoglycan

D

DOTAP: 1,2-dioleoyl-3-trimethylammonium-propane

DOPE: 1,2-dioleoyl-*sn*-glycero-3-phosphoethanolamine

DSPE: 1,2-distearoyl-*sn*-glycero-3-phosphoethanolamine

DMEM: Dulbecco's Modified Eagle's Medium

DNA: Deoxyribonucleic acid

E

EPC: Egg phosphatidylcholine

EBM-2: Endothelial Cell Basal Medium

F

FVII: Blood coagulation factor VIIa

FBS: Fetal bovine serum

FACS: Fluorescence activated cell sorting system

G

GAG: Glycoseaminoglycan

H

HBV: Hepatitis B Virus

HCC: Hepatocellular Carcinoma

HCV: Hepatitis C Virus

HSC: Hepatic stellate cell

^{3}H-CHE: ^{3}H-Cholesterylhexadecyl ether

I

ICAM-1: Intercellular Adhesion Molecule 1

ICAM-2: Intercellular Adhesion Molecule 2

IL-8: Interleukin-8

IP-10: Gamma-interferon inducible protein

L

LDL: Low density lipoprotein

LSEC: Liver sinusoidal endothelial cell

LP: Liposome

M

MALDI-TOF: Matrix assisted laser desorption/ionization-time of flight

MEND: Multi functional Envelop type Nano Device

MIG: Monokine induced by gamma-interferon

MMP-9: Matrix metalloproteinase-9

MW: Molecular weight

MS: Mass Spectroscopy

N

NHS: N-hydroxy succinimidyl

NK: Natural killer cell

NO: Nitric Oxide

P

PEG: Polyethylene glycol

PBS: Phosphate buffer saline

PEG-LP: PEGylated liposome

PECAM-1: Platelet endothelial cell adhesion molecule-1

pDNA: plasmid DNA

R

R8: Octaarginine

Rhodamine: N-(lissamine rhodamine B sulfonyl)

RILD: Radiation-Induced Liver Disease

S

STR-R8: Stearylated octaarginine

siRNA: small interfering RNA

SOS: Sinusoidal Obstruction Syndrome

V

vWF: Von Willebrand factor

VCAM-1: Vascular cell adhesion protein 1